

Object: Response to reviewers' comments on "Seasonal variation of ozone and black carbon observed at Paknajol, an urban site in the Kathmandu Valley, Nepal" by D. Putero et al.

Dear Editor,

Please find below our point-to-point replies (bold italic) to the specific comments raised by the two reviewers. We believe all comments have been addressed and we followed all suggested changes. Modifications as respect to the original manuscript are included in the new version uploaded, and marked with red color in the manuscript version below.

We thank the referees for their useful and valuable comments and we hope the manuscript now meets the journal's specific standards for publication.

Yours sincerely,

Davide Putero (on behalf of all the co-authors)

Reviewer #1:

The authors present measurements of BC (light absorption), ozone, and aerosol particles (PM1 and PM10) obtained over approximately a year in the Kathmandu Valley. The year is broken up into 4 periods, pre-monsoon, monsoon, post-monsoon, and winter. Diurnal pattern of the quantities measured appear to be typical of that found in many other locations, dominated by the time dependence of emissions, photochemistry, and boundary layer dynamics. There is some dependence of ozone on wind direction and the high ozone season coincides with the season for regional vegetation fires. What is present appears to be basically correct, though not very exciting because similar features have been seen before and with a limited suite of instruments there is only so much that can be said about cause and affect.

We thank the Reviewer for his/her valuable suggestions and his/her encouraging evaluation. In the following, we report our point-to-point replies to each of the raised points. Modifications to the text are performed in the revised version of the manuscript and are marked in red color.

The experimental setup was defined taking into account both the scientific goals of the SusKat campaign (i.e. achieving a more comprehensive understanding of the dynamics of air pollution and related emissions in the Kathmandu Valley, and constituting the scientific basis in order to support the local implementation of mitigation actions) and the complex logistic conditions in Kathmandu. Since a long duration experiment was planned, state-of-art instrumentation was selected, characterized by a well-known robustness and relatively low necessity of human interventions. It should be also kept in mind that the Kathmandu urban area is characterized by severe problems of power distribution and that black-out can often occur for several hours per day. Even though an UPS system was installed at Paknajol, the installation of complex instrumentation characterized by high power demand (e.g. AMS, SMPS/DMPS) was prevented.

However, to our knowledge, this experimental suite still represents the most complete setup ever installed at a single measurement site in the Kathmandu city center.

We believe that having kept these “basic” instruments running for almost two years up to date has been a success, useful for providing a unique dataset that can be used for the implementation of mitigation measurements.

An opportunity that is missed is the determination of relations between ozone, BC, and aerosol particles (accumulation and coarse mode). Correlations between these quantities are presented in Table 2, but because all data is used it is not possible to distinguish chemical effects from boundary layer dynamics. I suggest that this paper could interest a wider audience with a partial repeat of Table 2, limiting the data to convective hours. A very interesting quantity to look for is secondary aerosol production. Insight can be gained by looking at the regression of ozone vs. PM₁. Also BC vs. PM₁. I'm guessing that relations would be lost by doing regressions on a data subset defined by season or trajectory location. I would do regressions on a day by day basis and see what drops out. Perhaps the slopes of these plots will depend on solar radiation.

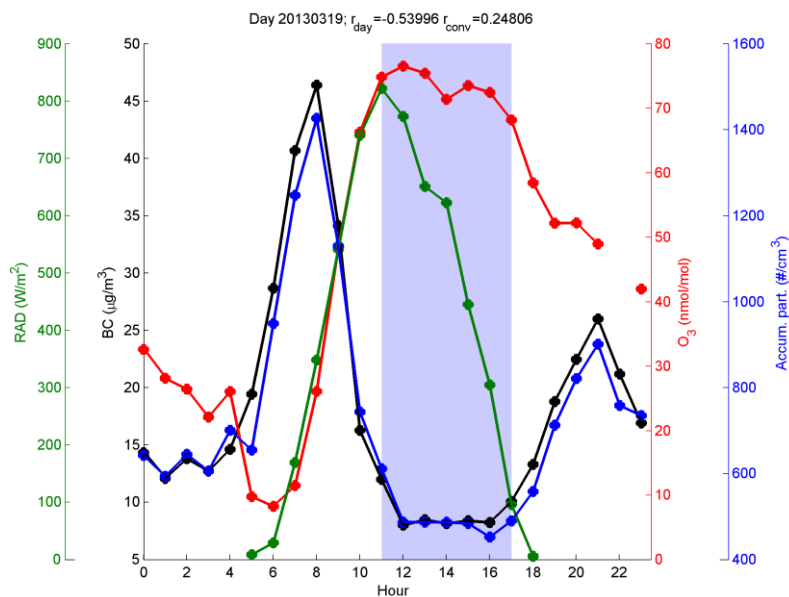
I recommend publication with revisions, though I believe the authors would be well served by seeing whether an approach such as given above is productive.

We thank the Reviewer for his/her perspicacious advice on performing correlations on a limited subset only. Unfortunately, our PM₁ values were collected on a daily basis (24h resolution), thus a direct comparison with a subset of O₃ or BC hourly values was not possible. Keeping also in mind that accumulation and coarse particles were available for two seasons only (pre-monsoon and monsoon), we added a new Table (Table S1, Supplement), where correlations are performed on a subset between 11:00 and 17:00 LT. This time range corresponds, according to the average diurnal variations for wind speed and solar radiation, to the convective hours. By looking at Table S1, the computed r between BC and the number of accumulation particles did not differ much from that of Table 2, indicating the important role of primary emissions (traced by BC) in determining aerosol particle number; nevertheless, the slight decrease in such correlation might indicate the presence of other processes (such as secondary aerosol production). This was further highlighted by the change in the correlation coefficient between O₃ and the accumulation fraction during the convective hours. O₃ can be considered a tracer of secondary pollution processes; moreover, as also shown in the paper, at Kathmandu the high O₃ values in the afternoon are the consequence of transport of aged air masses from the upper residual layers and/or horizontal advection.

Table S1. Correlation coefficients (r) between several parameters (BC, O_3 , accumulation and coarse particles, WS, T and RAD) for hourly and daily (in parentheses) values, over the whole sampling period, computed during convective hours only (i.e. between 11:00 and 17:00).

	O_3	BC	Acc.	Coarse	WS	T	RAD
O_3	-	0.20 (0.17)	0.62 (0.61)	0.51 (0.52)	0.16 (0.49)	0.18 (0.16)	0.50 (0.53)
BC	0.20 (0.17)	-	0.82 (0.81)	0.79 (0.71)	-0.35 (-0.24)	-0.44 (-0.58)	-0.10 (-0.36)
Acc.	0.62 (0.61)	0.82 (0.81)	-	0.79 (0.79)	-0.03 (0.15)	-0.13 (-0.13)	0.03 (-0.01)
Coarse	0.51 (0.52)	0.79 (0.71)	0.79 (0.79)	-	-0.06 (0.21)	-0.03 (0.03)	0.03 (0.04)
WS	0.16 (0.49)	-0.35 (-0.24)	-0.03 (0.15)	-0.06 (0.21)	-	0.28 (0.37)	0.11 (0.72)
T	0.18 (0.16)	-0.44 (-0.58)	-0.13 (-0.13)	-0.03 (0.03)	0.28 (0.37)	-	0.34 (0.50)
RAD	0.50 (0.53)	-0.10 (-0.36)	0.03 (-0.01)	0.03 (0.04)	0.11 (0.72)	0.34 (0.50)	-

Despite adding this new Table, we further analyzed, on a day-by-day basis, the diurnal variations for O_3 , accumulation particle number, BC and RAD. In the following, we report two case studies, very different one from each other. In the first case, we observed a situation dominated by primary pollution, as testified by the high correlation between BC and accumulation particles: for this case, the correlation between O_3 and accumulation particle number during the convective hours was fairly poor ($r = 0.25$). During the second analyzed day, we observed higher correlation ($r = 0.97$) between O_3 and the accumulation fraction. For this case, we supposed that aged air-masses richer in secondary pollutants (i.e. O_3 and aerosol) have been mixed and transported to the measurement site within the afternoon mixed layer.



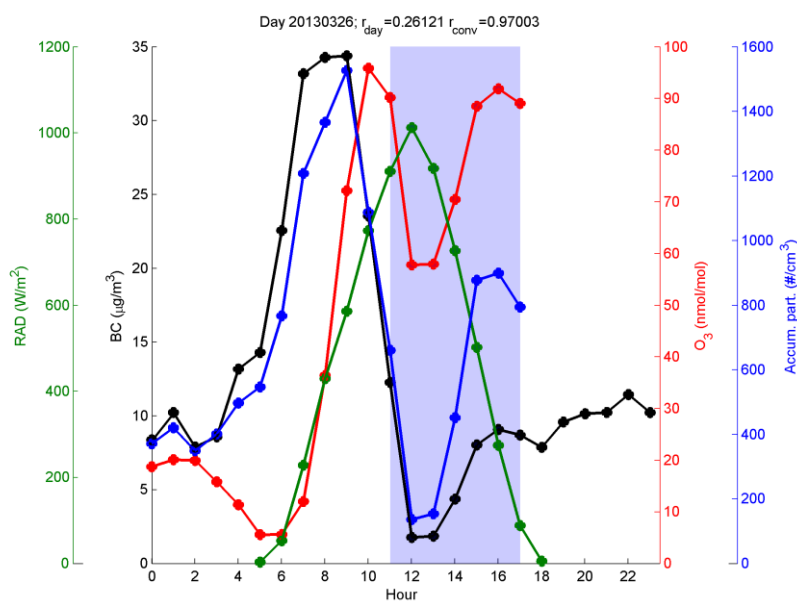


Figure R1. Diurnal variations for BC, O₃, accumulation particles and RAD, for two specific days: dominated by primary pollution (top) and likely influenced by other processes (bottom). Shaded areas represent the convective hours, i.e. between 11:00 and 17:00 LT.

The text was modified as follows (Page 22543, Line 23): “In order to distinguish the chemical effects from the boundary layer dynamics, we also computed correlation coefficients limiting the data to convective hours only (i.e. between 11:00 and 17:00, according to the wind speed and solar radiation diurnal variations). The slight weaker correlation between BC and accumulation particle number and, on the other hand, the increase in correlation between O₃ and accumulation particle number may indicate the role of other processes (e.g. secondary aerosol production) in the air-masses which characterize this specific time span (Table S1, Supplement). In particular, we suppose that aged air-masses rich in secondary pollutants (i.e. O₃ and aerosol) can be transported to the measurement site in the afternoon mixed layer.”

General Comments:

The paper presents many numerical values of concentration in the text. These numbers would be much easier for a reader to find if they were instead reported in a Table. I realize that there is a diversity of time periods and meteorological conditions, such that the number of Table headings could be unwieldy. I would urge the authors to select for a Table as large a subset as makes sense for comparisons and reserve for the text, a discussion of comparisons, etc.

We decided to insert a new Table, encompassing average and standard deviation values of the pollutants for every season, to decrease the amount of numerical values in the text and enhance its readability. Therefore, most of these numerical values have been removed in Section 3.2, where lines are now referring to Table 2 (Table 2 of the previous version of the manuscript has now become Table 3). Moreover, a new sentence has been added (Page 22537, Line 6): “...the seasons, while seasonal average values are presented in Table 2.”

Table 2. Average values (\pm standard deviation) of the pollutants, computed for the different seasons selected by the periods of Table 1.

	O ₃ (nmol/mol)	BC ($\mu\text{g}/\text{m}^3$)	Accum. ($\#/ \text{cm}^3$)	Coarse ($\#/ \text{cm}^3$)	PM ₁ ($\mu\text{g}/\text{m}^3$)	PM ₁₀ ($\mu\text{g}/\text{m}^3$)
Pre-monsoon	38.0 \pm 25.6	14.5 \pm 10.4	668 \pm 383	4.2 \pm 2.5	98 \pm 83	241 \pm 134
Monsoon	24.9 \pm 16.5	6.3 \pm 3.8	250 \pm 141	1.9 \pm 1.1	32 \pm 12	107 \pm 37
Post-monsoon	22.8 \pm 17.0	6.2 \pm 3.9	-	-	26 \pm 10	101 \pm 38
Winter	20.0 \pm 19.8	18.3 \pm 14.1	-	-	74 \pm 26	320 \pm 75
All	27.0 \pm 21.3	11.6 \pm 10.7	505 \pm 372	3.3 \pm 2.4	48 \pm 42	169 \pm 113

Page 22538, line 21-25. Ratio of daily to hourly standard deviations are an interesting quantity. However, I have not read Chevalier et al (2005) and don't know how to interpret these numbers other than the sweeping statement that daily and hourly variations are both important. A concern is that seasonal variations are clearly affecting BC and to a lesser extent ozone. A different way to look at data would be to use relative standard deviations that could be defined e.g., for the diurnal case by normalizing a day of measurements by the average of that day and for the daily case, normalizing by the average over a time period which could be a year or could be one of 4 periods defined or could be periods of defined length, such as a month.

By following Chevalier et al. (2007), the ratio daily/hourly variability aims at identifying what is the contribution of boundary-layer processes compared to that due to day-to-day changes (e.g. changing weather conditions, transport at synoptic scale) in determining O₃ and BC variations. Since no clear signal is obtained for what concerns O₃ and BC measurements (0.54 for O₃ and 0.59 for BC), we stated that both processes account the same in attributing these pollutants' variability. However, under the Reviewer's suggestion, we also computed relative standard deviations, i.e. defined by normalizing each hourly value by the daily average and each daily value by the seasonal average to which that day belongs. For BC, the relative standard deviations (daily/hourly) ratio is 0.54, thus almost equal to what obtained in the previous analysis; for O₃ it drops a bit more (0.42), further indicating the importance of diurnal photochemistry/local dynamics in determining O₃ variations at Kathmandu.

Regarding the conclusion that pollutants are mainly of local origin: This is further supported by the ratio of BC to PM₁. That ratio is too high to be due to wildland fires.

We agree with the Reviewer concerning this point. A new sentence has been added (Page 22548, Line 3): "...at Paknajol, further supported by the high ratio BC/PM₁."

Significant figures: Aerosol concentrations are given to 0.1 particle per cm³ out of a total of hundreds to more than a thousand. Actual accuracy is of order 10%. The decimal digit should at least be removed for values greater than 100.

This has been corrected. All decimal digits for accumulation particles and for PM concentrations have been removed.

Term "correlation coefficient": It appears from the negative values in Table 2 that you have followed correct usage and are reporting r, not r². It would be useful to have an explicit statement, which could be done as simply as adding (Pearson's r) or even (r) at the point first mentioned.

The expression “(r)” has been added in the new version of the manuscript (Page 22542, Line 24) and in the caption of Table 3.

Specific Comments:

Page 22532 - 22533 Are instrument averaging times for instruments described in bullets 1 to 4 given in text?

All instruments described in bullets 1 to 4 in Section 2.1 sample at 1-minute time resolution. Measurements are validated on a 1-min basis and then averaged in order to obtain hourly values. This is stated in Page 22534, Lines 1-3.

page 22532, line 24 “These are referred to the SRP15 reference scale ...” please explain.
SRP15 stands for Standard Reference Photometer 15. It is the instrument used within WMO/GAW to propagate the NIST ozone measurement scale. For clarification, the manuscript has been modified and a new reference has been added (Page 22532, Line 24): “These are referred to the WMO/GAW reference scale (SRP#15, see Klausen et al., 2003) hosted at the GAW World Calibration Centre (WCC) at EMPA (Switzerland)”.

Klausen, J, Zellweger, C, Buchmann, B, and Hofer, P, 2003. Uncertainty and bias of surface ozone measurements at selected Global Atmosphere Watch sites. Journal of Geophysical Research 108 (D19), 4622, doi:10.1029/2003JD003710.

page 22533, line 18 coincidence errors Are number concentrations high enough that coincidence errors are a concern? What was the maximum dilution factor used? Dilution flow rate is given but not sample flow rate.

The maximum concentration that avoids coincidence error is 500000 L^{-1} , as declared by the OPC manufacturer. The sample flow rate was kept constant at 1 L min^{-1} ; the highest dilution factor used was 5, even though the most used was 4 (being the dilution flow often 3 L min^{-1}) that thus raises the coincidence error limit to $2\cdot 10^6\text{ L}^{-1}$. This limit was exceeded rarely: only few hours at the end of March and at the beginning of April 2013. Therefore, we can consider negligible its impact on the dataset.

page 22534, line 25 recurrent neural network How does a recurrent neural network take into account the multi-day effects of meteorology? There is a reference but a simple explanation would aid the reader.

The Elman network used in this work is composed by three layers: the input layer, the hidden layer and the output layer. In the Elman network some nodes of the input layer are set with the status of the neurons in the hidden layer, in this way the signal is backpropagated from the hidden layer to the input layer. The effect is that the neurons in the second layer contain information of parameters at the previous time step. This mechanism takes into account the multi-day effects of meteorology. This information is fully presented in Biancofiore et al. (2015).

page 22535, line 4 meteorological effects usually last for more than one day You are implicitly defining meteorological effects to exclude diurnal boundary layer cycles.

Yes, the Reviewer is partially right: there are boundary layer cycles but also meteorological conditions that last for more than a day. In our model architecture, both are taken into account.

In the revised version of the manuscript we will highlight this point (Page 22535, Line 6): “...of meteorology, as well as diurnal boundary layer cycles”.

page 22538, line 26-27. Fig 3 shows the shape of the ozone diurnal cycle was similar during all seasons. I disagree. The pre-monsoon ozone is clearly different in the late afternoon.

This sentence was meant to highlight the fact that the maxima and minima in the O₃ diurnal cycle occurred at the same moment of the day, independently on the season. The sentence has been rephrased: “O₃ diurnal variation is shown in panel b of Fig. 3: a peak in O₃ mixing ratios characterized the central part of the day (between 11:00 and 13:00), while a minimum was observed in the morning (between 5:00 and 6:00).”.

page 22541, line 4 “We magnified ...” magnified is not the correct word. perhaps you call attention to something, but it is not made larger

The term “magnified” has been changed to “highlighted”.

page 22543 line 9, direct pollution What is the meaning of direct in this context? Term not commonly used as a synonym of emitted or primary.

The term “direct” has been changed to “primary”.

Page 22543 – 22544 Discussion of Fig. 6 hard to follow. Before I accept the conclusion that high ozone at 16:00 is due to dynamical effects (attributed to upper residual ozone in one place and residual ozone and/or horizontal advection in another place), I would want to see a diurnal cycle predicted using only RAD.

The different simulations reported in Fig. 6 show that, when in the model is used only wind speed as input data, the model simulates well only the afternoon high level of O₃, missing completely the peak before noon. In contrast, by modelling O₃ using as input parameters wind speed and solar radiation, the model reproduces well the peak before noon and the high levels of afternoon-evening O₃. Putting together the results of these two simulations, we can conclude that the high level of O₃ during the afternoon is mainly due to dynamics, for the following two reasons: (i) in the model, the wind speed used as input is enough to reproduce the afternoon concentrations of O₃ and (ii) the inclusion of solar radiation does not improve the agreement between measured and modelled O₃ during the afternoon, but enhances substantially the agreement between measurements and simulations before noon, when photochemistry, as expected, plays a larger role.

This paragraph has been rephrased to make this part clearer (Page 22543-22544, Lines 27-29 and 1-9): “The simulation that included all the proxies reproduced quite well the observed O₃ mixing ratios for all hours of the day, whereas a simulation that included only wind speed (a good proxy of atmospheric dynamics) reproduced with accuracy the afternoon (after 15:00) and evening levels of O₃, missing completely the main O₃ peak before noon. In contrast, by using as input parameters both wind speed and solar radiation, the model reproduced well the peak before noon and the high levels of afternoon-evening O₃. Putting together the results of these two simulations, we can conclude that the high level of O₃ during the afternoon is mainly due to dynamics (vertical intrusion from upper atmospheric layers and/or horizontal advection), for the following two reasons: (i) in the model, the wind speed used as input is enough to reproduce the afternoon concentrations of O₃ and (ii) the inclusion of solar radiation does not improve the

agreement between measured and modelled O₃ during the afternoon, but substantially enhances the agreement between measurements and simulations before noon, when photochemistry, as expected, plays a larger role.”

page 22546 line 8 much polluted regions please rephrase
The word “much” was a misprint, thus has been removed.

Table 9 Time axis. Split into hard-to-visualize intervals. Suggest monthly or bi-monthly ticks. A shading scheme in plot C that delineates 4 meteorological periods would help the reader follow text. *Figure 9 has been modified, by changing the x-axis using monthly ticks (same as Fig. 2). Moreover, in order to distinguish the different seasons, four shading areas have been added to panel c. Colors for these refer to the ones used in Figure 3. The caption has been modified accordingly.*

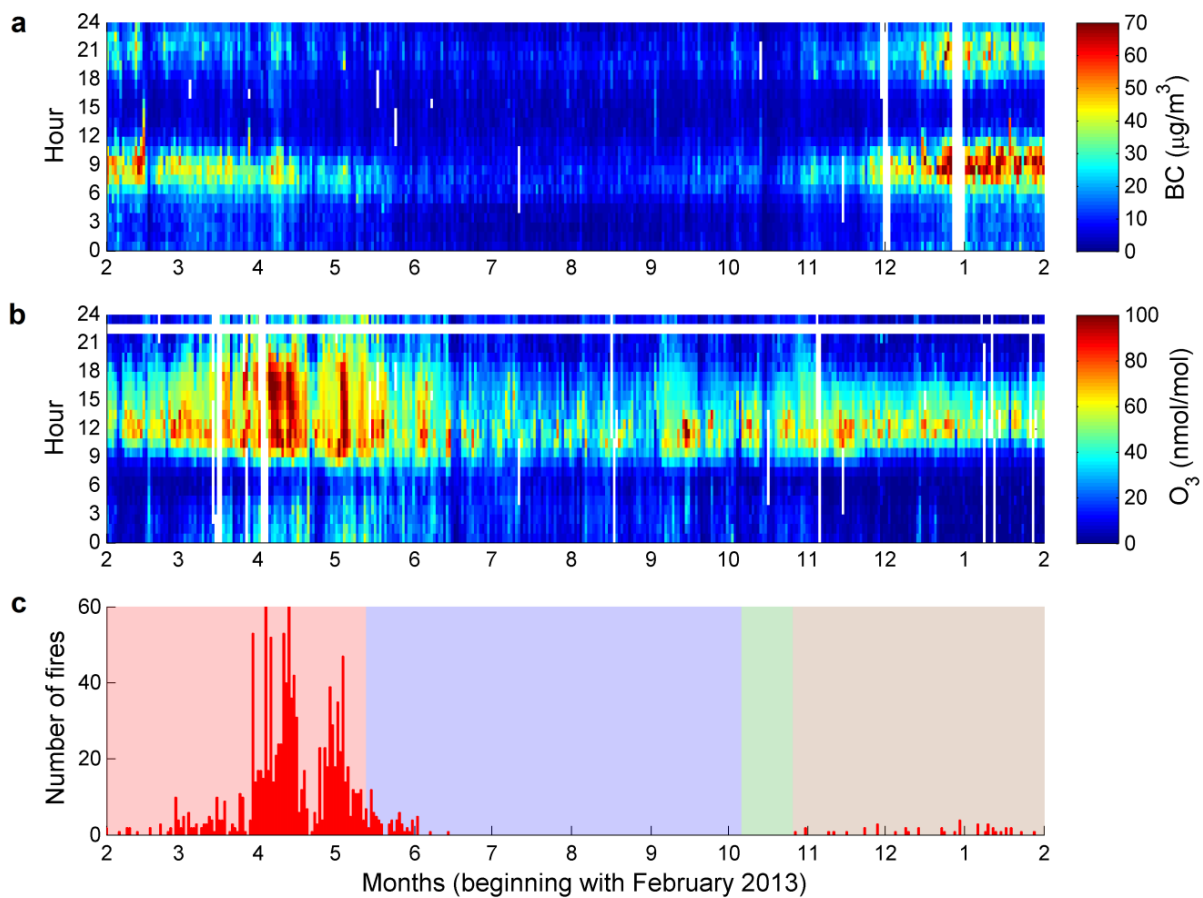


Figure 9. BC (panel a) and O₃ (panel b) diurnal variations over the entire sampling period. The color scale has been set to a maximum of 70 μg/m³ and 100 nmol/mol for BC and O₃, respectively. Panel c shows the total daily number of fires found in the Southern Himalayas box (see Putero et al., 2014); note that the y-axis has been limited to a maximum value of 60. Shaded areas in panel c indicate the different seasons (red: pre-monsoon, blue: monsoon, green: post-monsoon and brown: winter).

Reviewer #3:

General Comments:

Putero et al. present the first full year analysis of the simultaneous observations of the short lived climate forcers/pollutants ozone and black carbon (measured as equivalent black carbon) as well as aerosol number and mass concentration at a site in the center of the Kathmandu metropolitan city, Paknajol (Nepal). The measurements allow for a detailed analysis of seasonal and diurnal changes in the trace gas and aerosol concentration. The characteristics for the seasonal and diurnal cycles are linked to either local sources of pollution or larger scale processes (e.g. atmospheric circulation) compared for four different seasons, including pre-monsoon, monsoon, post-monsoon and winter. Local pollution sources are considered to be the major contributor to the observed in general very high levels of short lived climate forcers/pollutants that lead to persistent poor air quality conditions in Kathmandu. The authors propose these data to be very useful for implementing mitigation strategies for the occurrence of acute pollution levels. The paper is well written and the observations are discussed in sufficient details. I recommend publication after some revisions listed below.

We thank the Reviewer for his/her valuable suggestions and his/her encouraging evaluation. In the following, we report our point-to-point replies to each of the raised points. Modifications to the text are performed in the revised version of the manuscript and are marked in red color.

Specific comments:

1) page 22534, line 1 ff: Was the start point (initial coordinates) for the 5 days back trajectories only located at the measurement site itself or did the authors consider calculating back trajectories on a grid at different altitudes around the measurement station (variation of the initial coordinates) to increase the confidence for the results in the complex topography besides choosing the start altitude at 600 hPa to account for the complex terrain?

In our analysis we considered several sets of back-trajectories, starting at different altitudes above the measurement station (i.e. 500, 1500 and 2000 m a.g.l.). The final choice of retrieving only those starting at roughly 600 hPa was made because the lower ones were often impacting the complex orography that characterizes the area around the measurement site. Moreover, it has to be noted that in this work we used isentropic (and thus not kinematic) back-trajectories: this because, taking into account the large uncertainties which can affect back-trajectory analysis based on “global” meteorological data like GDAS in a complex topography, we were mainly interested in understanding the impact of large-scale meteorological scenarios (and related atmospheric circulation) to the atmospheric composition variability in Kathmandu, rather than attributing the exact source regions to each cluster.

2) page 22538, line 6: It would be helpful to list some details on the meteorological component contributing to a morning return of pollutants.

The mechanisms contributing to the morning return of pollutants are fully explained in Panday and Prinn (2009) and Panday et al. (2009). Basically, during night-time, the radiative cooling of mountains (i.e. the Kathmandu Valley’s flanks) generates downslope (katabatic) winds, which establish a flow of cold air towards the basin bottom. These parcels of relatively cold air flow underneath the less cold and less dense (but also more polluted) air mass which is already present, consequently lifting this “polluted air-mass pool” above. The rising of this polluted air-mass is active along the night (causing thus a night-time minimum in pollutants at surface, see

Figure 3), as the cold and cleaner air masses keep on descending from the valley flanks. In the early morning, the mixed layer starts to grow, causing the downward mixing of such polluted air-mass back to the city.

We included a brief description of this phenomenon in the text, by modifying as follows (Page 22538, Line 6): “Moreover, also a meteorological component cannot be ignored: this is due to the presence of katabatic winds that lead to the uplift of surface polluted air-masses during the night. The following build-up of the morning mixed layer favors the downward mixing of pollutants back to the valley’s bottom (Panday and Prinn, 2009; Panday et al., 2009).”.

3) page 22541, line 1-2: What is the reason for the PM₁/PM₁₀ ratio being generally higher in European cities? A reference for this statement would be helpful.

The main reason impacting the PM₁/PM₁₀ ratio in the Asian cities is the higher presence of dust in the roads (being also a lot of them unpaved, e.g. in Kathmandu), leading to higher dust resuspension in the latter ones, with respect to the European cities. We did not find a reference comparing European and Asian cities; nevertheless, many papers reported values of 0.56-0.71 in Milan -Italy- (Giugliano et al., 2005), 0.5-0.6 in Vienna -Austria- (Gomiscek et al., 2004), and 0.33-0.42 in Athens -Greece- (Theodosi et al., 2011).

Giugliano, M., Lonati, G., Butelli, P., Romele, L., Tardivo, R., and Grosso, M., 2005. Fine particulate (PM_{2.5}–PM₁) at urban sites with different traffic exposure. Atmospheric Environment 39(13), April 2005, Pages 2421–2431.

Gomiscek, B., Hauck, H., Stopper, S., and Preining, O., 2004. Spatial and temporal variations of PM₁, PM_{2.5}, PM₁₀ and particle number concentration during the AUPHEP—project. Atmospheric Environment 38, 3917–3934.

Theodosi, C., Grivas, G., Zarmas, P., Chaloulakou, A., and Mihalopoulos, N., 2011. Mass and chemical composition of size-segregated aerosols (PM₁, PM_{2.5}, PM₁₀) over Athens, Greece: local versus regional sources. Atmospheric Chemistry and Physics 11, 11895–11911.

4) page 22544, line 5 ff: The authors use a recurrent neural network model to distinguish between contributions from photochemistry and dynamics to the observed O₃ mixing ratio. Does this analysis allow for a more detailed budget analysis for ozone leading to absolute and relative numbers for the contribution of the different processes which can be included in this section?

We thank the Reviewer for this suggestion. Comparing the simulation that uses as inputs in the model all the parameters with the simulation that includes only wind speed as input data (see Fig. 6), we can conclude that photochemistry contribution varied as a function of the hour of the day, ranging from 6% to 34%. Two new sentences have been added to the paper: (Page 22544, Line 9) “The photochemistry contribution varied as a function of the hour of the day, ranging from 6% to 34%.” and (Page 22549, Line 2) “photochemistry (which contribution ranges from 6% to 34%)”.

5) page 22548, line 7 ff: What are the timescales for the transport of the polluted air masses to the measurement region? For example Roelofs et al., 1997 and Andreae et al., 2001 report ozone production rates of 10 ppbv/day and higher in air masses affected by biomass burning emissions. Are the transport timescales long enough for sufficient ozone production to explain the O₃ enhancement observed in the diurnal cycles?

In this work we specifically considered only fires occurring in the Southern Himalayas (SHI) box ([26, 30]x[80, 88]), considered the main area for open fire emissions contributing to O₃ and BC variability in Nepal (Putero et al., 2014). In that work the emission age (in hours) during wildfires was estimated, resulting 1.8 days on average; moreover, for 50% of the analyzed cases the last active fire had been overpassed by air-masses in the last 24h before reaching the measurement site. In our analysis we observed that, for WES and REG clusters (which were the most occurring during wildfire events) the transport timescale was comprised mostly within 24h. With all of this information, we can conclude that it is sufficient for explaining the O₃ enhancement. However, it has to be noted that the O₃ production from wildfires is a tricky process which may have different timescales, since it involves several variables, such as fire emissions, chemical and photochemical reactions, aerosol effects on chemistry and radiation, local and downwind meteorological patterns, as fully explained in Jaffe and Wigder (2012).

Jaffe, D.A., and Wigder, N.L., 2012. Ozone production from wildfires: a critical review. Atmospheric Environment 51, 1-10.

Technical corrections:

page 22529, line 13: ...the analysis of seasonal changes of the diurnal cycles and the correlation...
(?)

page 22529, line 15: ...during the afternoon/evening. This could be related...

page 22530, line 24: ...during the period 2005 -2015. By 2015, there...

page 22532, line 9: ...As reported by Panday and Prinn (2009) and Panday et al. (2009)...

page 22532, line 21: ...measurement activities, including aerosol and trace gas measurements, were started...

page 22532, line 23: ...UV-absorption analyser...

page 22536, line 36: ...shown in Panday and Prinn (2009) and Panday et al. (2009),...

page 22537, line 18: ...what is reported in a previous study...

page 22540, line 11: ...than those of Giri et al. (2006). This is...

page 22540, line 26: ...dust outbreak episodes (Alastuey et al., 2005) and dusty roads...

page 22541, line 9: ...These analysis refer to...

page 22541, line 24: ...and aerosol particles...

page 22547, line 6: ...Friedl et al., 2010). This methodology...

page 22548, line 22: ...opposite to what was observed...

page 22549, line 1: ...the analysis of the seasonal change of the diurnal cycle... (?)

page 22550, line 7: ... guidelines for O₃ (?) based...

All of these technical corrections have been applied in the revised version of the manuscript.

Seasonal variation of ozone and black carbon observed at Paknajol, an urban site in the Kathmandu Valley, Nepal

D. Putero¹, P. Cristofanelli¹, A. Marinoni¹, B. Adhikary², R. Duchi¹, S. D. Shrestha³, G. P. Verza⁴, T. C. Landi¹, F. Calzolari¹, M. Busetto¹, G. Agrillo¹, F. Biancofiore⁵, P. Di Carlo⁵, A. K. Panday², M. Rupakheti⁶, and P. Bonasoni¹

[1] {CNR-ISAC, National Research Council of Italy - Institute of Atmospheric Sciences and Climate, Via Gobetti 101, 40129, Bologna, Italy}

[2] {ICIMOD, International Centre for Integrated Mountain Development, G.P.O. Box 3226, Khumaltar, Lalitpur, Kathmandu, Nepal}

[3] {Ev-K2-CNR Committee, G.P.O Box 5109, Paknajol, Kathmandu, Nepal}

[4] {Ev-K2-CNR Committee, Via S. Bernardino 145, 24126, Bergamo, Italy}

[5] {Center of Excellence CETEMPS, University of L'Aquila, Via Vetoio 1, 67010, Coppito (AQ), Italy}

[6] {IASS, Institute for Advanced Sustainability Studies, Berliner Strasse 130, 14467, Potsdam, Germany}

Correspondence to: D. Putero (d.putero@isac.cnr.it)

Abstract

The Kathmandu Valley in South Asia is considered as one of the global “hot spots” in terms of urban air pollution. It is facing severe air quality problems as a result of rapid urbanization and land use change, socioeconomic transformation and high population growth. In this paper, we present the first full year (February 2013 – January 2014) analysis of simultaneous measurements of two short-lived climate forcers/pollutants (SLCF/P), i.e. ozone (O_3) and equivalent black carbon (hereinafter noted as BC) and aerosol number concentration at Paknajol, in the center of the Kathmandu metropolitan city. The diurnal behavior of equivalent black carbon (BC) and aerosol number concentration indicated that local pollution sources represent the major contributions to air pollution in this city. In addition to photochemistry, the planetary boundary layer (PBL) and wind play important roles in determining O_3 variability, as suggested by **the analysis of seasonal changes of the diurnal cycles and the correlation** with meteorological parameters and aerosol properties. Especially during pre-monsoon, high values of O_3 were found **during the afternoon/evening. This could be related** to mixing and entrainment processes between upper residual layers and the PBL. The high O_3 concentrations, in particular during pre-monsoon, appeared well related to the impact of major open vegetation fires occurring at regional scale. On a synoptic-scale perspective, westerly and regional atmospheric circulations appeared to be especially conducive for the occurrence of the high BC and O_3 values. The very high values of SLCF/P, detected during the whole measurement period, indicated persisting adverse air quality conditions, dangerous for the health of over 3 million residents of the Kathmandu Valley, and the environment. Consequently, all of this information may be useful for implementing control measures to mitigate the occurrence of acute pollution levels in the Kathmandu Valley and surrounding area.

1. Introduction

Air pollution is a major environmental challenge in several regions of the world, defined as “hot spots” (Monks et al., 2009). In South Asia, by using in situ measurements, chemical transport models and satellite observations, Ramanathan et al. (2007) identified layers of regional-scale plumes of atmospheric pollutants that extended from the Himalayas to the northern Indian Ocean, including high levels of short-lived climate forcers/pollutants (SLCF/P), such as black carbon (BC) and ozone (UNEP and WMO, 2011). Several significant implications of these compounds were recognized for the global climate (Ramanathan and Carmichael, 2008), regional climate and crop yields, and for human health (Shindell et al., 2012).

The Kathmandu Valley in Nepal, the largest metropolitan region at the Himalayan foothills (one of the most polluted but still least sampled regions of the world), represents one of the regional hot spots in terms of air pollution. This area, having a cross section of about 20 km north to south and 30 km east to west, comprises of three administrative districts, Kathmandu, Lalitpur and Bhaktapur, and has undergone rapid but unplanned urbanization due to high population growth, dramatic land use changes and socioeconomic transformation, thus facing severe air pollution problems. Over the past quarter century the Kathmandu Valley’s population has quadrupled to more than 3 million. Between 1990 and 2014 the total vehicle fleet grew from 45,871 to more than 700,000, with the number of motorcycles having the highest annual growth rate of 16% during the period (Faiz et al., 2006; Shrestha et al., 2013). Furthermore, by using an energy system model, Shrestha and Rajbhandari (2010) indicated that the total energy consumption in the Kathmandu Valley will grow at an average growth rate of 3.2% **during the period 2005-2050. By 2050, there** will be an increase in the energy consumption of 30%, 25% and 22% for the shares of transport, industrial and commercial sectors, respectively. In the Kathmandu city center the air quality is so bad that Nepal’s own national ambient air quality standards are only met on about 40 days per year; during the rest of the period the particulate matter exceeds the limit considered harmful. The Kathmandu Valley sizable emission of air pollutants is of concern for local and regional air quality and climate; however, it is still a manageable size in terms of potential interventions to address serious air pollution problems in the valley. The relative importance of local and regional emission sources has not been well quantified yet, making it difficult to design mitigation strategies that will have a large impact and still be cost-effective. Therefore, an improved scientific understanding of the main sources and impacts of air pollution in the region is a prerequisite for designing effective mitigation options.

In the recent past, several studies have presented measurements of various atmospheric compounds in the Kathmandu Valley (e.g. Sharma et al., 2012; Panday and Prinn, 2009; Panday et

al., 2009; Pudasainee et al., 2006; Giri et al., 2006; Sharma et al., 1997; Shrestha and Malla, 1996), all suggesting that air pollution in Kathmandu has harmful effects on human health (leading to bronchitis, throat and chest diseases), crop productivity and also tourism income in Nepal, being Kathmandu the heart of the Nepalese culture, art and architecture. However, none of them presented simultaneous observations of key SLCF/P across seasons.

In order to provide continuous measurements of atmospheric composition variability, a measurement site was installed in 2013 at Paknajol, the tourist old area of the Kathmandu city. This has enabled us to achieve a more comprehensive understanding of the dynamics of air pollution and related emissions in the Kathmandu Valley, and to constitute the scientific basis in order to support the local implementation of mitigation actions. These measurements were carried out as part of the SusKat-ABC (A Sustainable Atmosphere for the Kathmandu Valley – Atmospheric Brown Cloud) campaign in Nepal, the second largest international air pollution measurement campaign ever carried out in southern Asia, which aim is to provide the most detailed air pollution measurements to date for the Kathmandu Valley and the surrounding region (Rupakheti et al., 2015).

2. Materials and Methods

2.1 Measurement site and instrumental setup

Kathmandu city is located in a broad basin at the foothills of the central Himalayas, with valley floor at an average altitude of 1300 m a.s.l. The mountains surrounding the valley have peaks ranging from 2000 to 2800 m a.s.l. Neighboring valleys to the west, north, northeast and south have substantially lower elevations. The Kathmandu Valley's meteorology is influenced by large scale features, western disturbances and the South Asian Summer Monsoon, as well as local mountain-valley circulations. **As reported by Panday and Prinn (2009) and Panday et al. (2009)** during the dry season the diurnal cycle of air pollutants (CO, O₃, PM₁₀) is strongly affected by local meteorology connected to the evolution of the convective planetary boundary layer (PBL) and thermal wind flows along the flanks of the mountains surrounding the valley.

The Paknajol site is located (27°43'4" N, 85°18'32" E, 1380 m a.s.l.) near the edge of Kathmandu's tourist district of Thamel. The sampling site stands on the terrace (about 25 m a.g.l.) of the Ev-K2-CNR representative office. This is the highest building in the block, thus having a 360° free horizon of at least 300 m. The instruments are located in an air-conditioned room, in order to maintain the correct operating conditions; an UPS for uninterruptible power supply guarantees the continuous measurements in case of (frequents) blackout events, up to 18 hours a day power cut, especially during the winter months. The sampling heads are placed on the roof just outside this

room. The measurement activities, including aerosol and trace gas measurements, were started on February 2013.

The following instruments are used for continuous measurements:

1. UV-absorption analyser (TEI 49i, Thermo Environmental) is used to collect surface O₃ measurements. These are referred to the WMO/GAW reference scale (SRP#15, see Klausen et al., 2003) hosted at the GAW World Calibration Centre (WCC) at EMPA (Switzerland), via direct comparison with the CNR-ISAC laboratory standard hosted at the Mt. Cimone WMO/GAW Global Station (Italy). The experimental setup is similar to that described in Cristofanelli et al. (2010).
2. Aerosol light absorption and BC, derived by using the mass absorption efficiency of 6.5 m² g⁻¹, are measured through a Multi-Angle Absorption Photometer (MAAP 5012, Thermo Electron Corporation). For more details, see Marinoni et al. (2010). The correction described in Hyvärinen et al. (2013) for the measurement artifact, affecting the instrument's accuracy at high BC concentrations, was applied. A PM₁₀ cutoff size was used in the sampling head.
3. Meteorological parameters (atmospheric pressure and temperature, wind speed and direction, relative humidity and precipitation) are monitored using an automatic weather station (WXT 425, VAISALA). Global solar radiation is monitored with a pyranometer (CMP21, Kipp&Zonen).
4. Aerosol number concentration and size distribution (in the range 0.28 μm ≤ D_p < 10 μm, D_p being the geometric diameter of particles) are measured using an Optical Particle Counter (OPC Monitor, FAI Instruments), which uses laser light scattering technique (λ=780 nm). The OPC optical diameters (divided in 8 bins) are then converted into geometric diameters, assuming that particles are spherical. In order to minimize biases related to coincidence errors, but also to reduce relative humidity and dry aerosol particles, the air sample is subjected to a dilution process, whose dilution factor can be varied, by modifying the dilution flow rate (from 0 to 4 l/min).
5. On-line PM₁₀ and PM₁ are measured (with a 24 h resolution), using the β-absorption technique, with a medium-volume (2.3 m³/h) sampler (SWAM Dual Channel, FAI Instruments). The instrument is equipped with two 12V back-up batteries, in order to complete measurements in case of electricity power breaks. From April 1st 2013 a PM₁ sampling head has been installed, replacing the PM_{2.5} one.

All measurements presented in this work refer to Nepal Standard Time (NST, UTC+05:45); data are stored and fully validated on a 1-min basis, then averaged to a common time base of 60 minutes, and expressed in STP (0 °C and 1013 hPa) conditions. With the purpose of aggregating

data to hourly average values, 50% data coverage criteria was used, i.e. at least 50% coverage of the data sampling period was required to give a 1-h average.

2.2 Back-trajectories calculation

In order to describe the synoptic-scale atmospheric circulation scenarios over the Kathmandu Valley and the surrounding region, the isentropic 5-days back-trajectories have been used, computed by the HYSPLIT model (Draxler and Hess, 1998) every 6 h (at 5:45, 11:45, 17:45 and 23:45 NST). With the aim of minimizing the effect of the complex topography and provide a description of the large-scale circulation in the free troposphere, calculations were initialized at 600 hPa. The model calculations are based on the GDAS meteorological field produced by the NCEP reanalysis data, with a horizontal resolution of $1^\circ \times 1^\circ$. In order to aggregate the back-trajectories of common origin, and better characterize the synoptic-scale circulation occurring at Paknajol, a cluster aggregation technique (Draxler, 1999) has been applied to the back-trajectories. Basically, at each step of the process, the appropriate number of clusters was identified, based on the variations of several statistical parameters; by maximizing between-group variance and minimizing within-group variance, this methodology might identify similar air-mass back-trajectories and aggregate them.

2.3 Recurrent model analysis

To understand how photochemistry and dynamics affect the variation of O_3 mixing ratios and to comprehend the origin of elevated O_3 levels in the afternoon and evening hours during the pre-monsoon period, we used a recurrent neural network model. These models allow us to simulate the non-linear relationship between O_3 and meteorological parameters that are proxies of photochemistry and dynamics (Lönblad et al., 1992; Elman, 1990). Considering the strong role of meteorological conditions and photochemistry on the variations of O_3 mixing ratios (Pudasainee et al., 2006; Di Carlo et al., 2007) and the fact that meteorological effects usually last for more than one day, the more complex architecture of the neural network that uses the recurrent approach takes into account the multi-day effect of meteorology, **as well as diurnal boundary layer cycles** (Biancofiore et al., 2015). The model uses the observed pressure, temperature, relative humidity, solar radiation, wind velocity and direction and BC concentrations as input to simulate the O_3 mixing ratio (Biancofiore et al., 2015). The inclusion of a sub-group of these proxies allows us to distinguish between the role of dynamics and that of photochemistry in the observed variations of O_3 mixing ratio.

3. Results

3.1 Meteorological characterization

The Paknajol area is strongly influenced by local traffic and urban emissions, as it is located near the edge of Kathmandu's tourist center, and near a major thoroughfare. Meteorological observations at the sampling site help in better describing the seasonal and diurnal variability of the air pollutants and SLCF/P in the Kathmandu Valley.

With the aim of identifying the regional transition of the monsoon seasonal regimes, we considered meteorological observations carried out at the Nepal Climate Observatory-Pyramid (NCO-P) station, located at 5079 m a.s.l. near Mt. Everest in the Himalayas. As shown by Bonasoni et al. (2010), the variability of meteorological parameters (i.e. relative humidity and meridional wind component) observed at NCO-P can be used to derive the onset and withdrawal dates of the different seasons on the south side of the Himalayan range (where NCO-P is located). Moreover, as described in the annual report of the India Meteorological Department (IMD, 2014), the seasonal advance of the South Asian monsoon cycle did not differ too much between NCO-P location and Kathmandu. Table 1 reports the start and withdrawal dates of each season (pre-monsoon, monsoon, post-monsoon, winter) for the period considered in this study.

Figure 1 shows the variability of the meteorological parameters measured at Paknajol from February 2013 to the end of January 2014. Hourly atmospheric temperature (T , panel *a*) values never exceeded 29.5 °C, while minima never dropped below 3.5 °C. Over the whole measurement period, T had an average value of 18.7 ± 5.6 °C (hereinafter, average values are indicated as average \pm one standard deviation). T was characterized by an evident diurnal cycle, with values peaking in the central part of the day and a minimum in the early morning. Atmospheric pressure (P , panel *b*, average value: 865.3 ± 4.1 hPa) showed its minimum values during the summer season, which is characterized by the presence of the monsoon trough over Nepal, accompanied by frequent and intense showers, reaching up to 47 mm/h (panel *d*). P is characterized by a semi-diurnal cycle, with two minima (at 4:00 and 16:00) and two maxima (at 10:00 and 22:00) with average amplitudes ranging from 1.2 hPa (pre-monsoon) to 3.5 hPa (post-monsoon). Relative humidity values (RH , panel *c*, average value: 67.1 ± 17.0 %) were high during all of the measurement period, rarely decreasing below 20% (50% during the summer monsoon season); it has to be noted that, during winter, RH values swing from very high to very low, thus presenting the widest diurnal cycle among all of the seasons. Saturation conditions (RH equal to 95% or higher) were mainly reached during the most intense rainfalls. In agreement with rainfall reported in Panday and Prinn (2009), about 90% of annual rainfall was observed during June-August. Panels *e* and *f* show wind speed and direction, respectively. The sampling site was characterized by low wind speeds, with majority of

winds from the W-NW sector, with secondary contribution from the W-SW sector (see Fig. S1, Supplementary Material). As shown in Panday and Prinn (2009) and Panday et al. (2009), nights were characterized by low wind speeds (maximum speed: 4 m/s) coming from several directions, mainly explained by katabatic winds descending from the mountain slopes at the edge of the Kathmandu Valley rim; on the other hand, during the afternoon, stronger winds (reaching up to 6.5 m/s) occurred at the measurement site, which was swept by westerly/northwesterly winds entering through the western passes.

3.2 SLCF/P seasonal and diurnal cycle

The hourly average (along with daily averages) time series for O₃, BC and particle number concentration are shown in Fig. 2. Figure 3 shows the diurnal variability of these pollutants across the seasons, while seasonal average values are presented in Table 2.

Similarly to other polluted cities, the rush hours and PBL dynamics result in the distinct morning and evening peaks: increase in traffic activities and congestion, increase in emissions from cooling/heating activities (LPG, kerosene and firewood), as well as decrease in PBL. The primary emission indicators, i.e. BC and aerosol particle number, reveal such activities. Industries, especially brick kilns, and open garbage burning also contribute to poor air quality in the Kathmandu Valley.

The average value of BC (Fig. 2, panel *a*) over the whole measurement period was $11.6 \pm 10.7 \mu\text{g}/\text{m}^3$. The highest BC concentrations were observed during pre-monsoon and winter seasons (Table 2), with daily values often exceeding $20 \mu\text{g}/\text{m}^3$, while the lowest values occurred during the monsoon season (the lowest daily value recorded was $2.5 \mu\text{g}/\text{m}^3$). These levels are slightly higher than what is reported in a previous study by Sharma et al. (2012) at Pulchowk Campus, in which they reported an average BC of $8.4 \pm 5.1 \mu\text{g}/\text{m}^3$, over a year-long study period spanning between May 2009 and April 2010. Another study by Shrestha et al. (2010) reported far lower values of EC concentration ($1.7 \pm 0.6 \mu\text{g}/\text{m}^3$) for an urban site 30 km southeast (downwind) of the Kathmandu Valley, during the 2009 pre-monsoon season. The highest seasonal values, observed during winter/pre-monsoon, can be attributed to several factors: increase in emissions from domestic heating, use of small but numerous gensets during extended hours with power cuts, operation of over 100 brick kilns in the Valley, refuse burning, as well as lower PBL and lower wet deposition of pollutants in winter months compared to the summer months with intense heat and rainfall. The average diurnal variation in BC concentrations in the different seasons is shown in Fig. 3, panel *a*. The typical diurnal variation for BC, as also shown in Sharma et al. (2012), reflects the BC profile for an urban site, presenting two daily maxima, with a prominent peak in the morning (between

7:00 and 8:00), and a second one in the evening (between 20:00 and 21:00), as well as two minima at night (between 1:00 and 2:00) and in the afternoon (between 14:00 and 15:00). These two daily peaks reveal the start and build-up of emissions due to local anthropogenic activities, such as traffic and cooking activities. **Moreover, also a meteorological component cannot be ignored: this is due to the presence of katabatic winds that lead to the uplift of surface polluted air-masses during the night. The following build-up of the morning mixed layer favors the downward mixing of pollutants back to the valley's bottom (Panday and Prinn, 2009; Panday et al., 2009).** This diurnal cycle was observed in all four seasons but the peak values were much higher in winter and pre-monsoon seasons (morning peaks: 41.4 and 33.3 $\mu\text{g}/\text{m}^3$, respectively) compared to the post-monsoon and monsoon seasons (12.9 and 11.4 $\mu\text{g}/\text{m}^3$, respectively).

Surface ozone (O_3) had an average value of 27.0 ± 21.3 nmol/mol (1 nmol/mol is equivalent to 1 ppb) over the whole measurement period (Fig. 2, panel *b*). The highest O_3 was observed during the pre-monsoon season, while the lowest values were reached during the winter season (Table 2). This spring “peak” is a feature widely present on South Asia and Himalayas (see e.g. Cristofanelli et al., 2010; Agrawal et al., 2008). Pudasainee et al. (2006), with measurements made at Lalitpur, an adjacent city to the Kathmandu municipality, suggested that variations of solar radiation, ambient temperature and precursors (such as NO_x and VOCs) can together explain 93% of the variation in measured ground level O_3 at Kathmandu. Following Chevalier et al. (2007), with the aim of attributing the fraction of O_3 , BC, accumulation and coarse particles variability related to day-to-day and diurnal scale processes, we calculated the ratio of daily/hourly standard deviations. The obtained values (0.54 for O_3 , 0.59 for BC, 0.81 for accumulation and 0.71 for coarse particles) indicated that both diurnal and day-to-day variations are important to explain O_3 , BC and particle number variations at Paknajol. **O_3 diurnal variation is shown in panel *b* of Fig. 3: a peak in O_3 mixing ratios characterized the central part of the day (between 11:00 and 13:00), while a minimum was observed in the morning (between 5:00 and 6:00).** This diurnal variation is typical for polluted urban sites (Jacobson, 2002) and can be explained in terms of local O_3 photochemistry production and removal processes as well as PBL dynamic and vertical air-mass mixing, as discussed in Sect. 3.4.

Particle number concentrations of accumulation ($0.28 \mu\text{m} \leq D_p < 1 \mu\text{m}$) and coarse ($1 \mu\text{m} \leq D_p < 10 \mu\text{m}$) particles are reported in Fig. 2 (panels *c* and *d*, respectively). Unfortunately, due to instrumental failures, no measurements were available after July 27th, 2013: only two seasons were covered, i.e. pre-monsoon and monsoon. The average values over the available time period were $505 \pm 372 \text{ cm}^{-3}$ for the accumulation particles and $3.3 \pm 2.4 \text{ cm}^{-3}$ for the coarse particles. Accumulation and coarse particle concentrations were high during the pre-monsoon season and far

lower during the monsoon (Table 2). The average seasonal diurnal cycles (Fig. 3c for accumulation and 3d for coarse) were somewhat similar to that of BC, presenting two daily peaks, in correspondence to the start of working activities and traffic rush, thus indicating common anthropogenic emission sources and similar meteorological influences. The similar behavior between accumulation and coarse particle number concentrations suggests likely common origins, indicating that the main fraction of coarse particle is linked to the resuspension of road dust or ash from local combustion and not to mineral dust transport from desert areas. During the pre-monsoon, the morning peak was higher (1054 cm^{-3} for accumulation and 7.4 cm^{-3} for coarse) than the one recorded in the evening (629 cm^{-3} and 4.3 cm^{-3} , respectively). The same was true for the accumulation mode even during the monsoon season, although the difference between the two peaks showed smaller amplitude. For coarse particles, however, the evening peak appeared to be higher than the morning peak during the wet season. This can be explained by considering the wet conditions which usually characterized Kathmandu during night-time along this season; moreover, it has to be noted that this phenomenon may be combined to a not sufficient aerosol drying from the dilution system of the OPC. Most of the rain occurs during the night-time and the wet surface in the early morning prevents emission of roadside dust and soil. As the day evolves, moisture is more efficiently evaporated, leaving dry dust and soil to be resuspended by traffic or winds, thus leading to the appearance of a larger evening peak for coarse particle number.

Figure 4 shows the seasonal box and whiskers plot for PM_{10} and PM_1 collected at Paknajol. Prior to April 1st 2013, a $\text{PM}_{2.5}$ sampling head was installed in place of the PM_1 one. By considering the whole sampling period, PM_{10} had an average value of $169 \pm 113 \text{ } \mu\text{g}/\text{m}^3$, which is comparable to the value found by Giri et al. (2006), $133.7 \pm 70.3 \text{ } \mu\text{g}/\text{m}^3$, computed over the period 2003-2005 for the Thamel measurement site (not far from Paknajol), or to the values found in Aryal et al. (2008), which range from 170 to $230 \text{ } \mu\text{g}/\text{m}^3$ (annual averages) for two busy traffic area stations in Kathmandu. Our value appears slightly higher than those of Giri et al. (2006). This is in line with the increasing urbanization and vehicles growth which occurred in the Kathmandu Valley. The maximum seasonal average of PM_{10} was found during winter, while minima occurred during monsoon and post-monsoon seasons (Table 2). $\text{PM}_{2.5}$ presented an average value of $195 \pm 83 \text{ } \mu\text{g}/\text{m}^3$ over its short time period (17 days), while PM_1 had an average value of $48 \pm 42 \text{ } \mu\text{g}/\text{m}^3$, with the maximum values during the pre-monsoon and winter seasons and significantly lower values during monsoon and post-monsoon (Table 2). Over the whole measurement period, the ratio $\text{PM}_1/\text{PM}_{10}$ was 0.29 ± 0.10 , indicating a large contribution of coarse particles to the total aerosol mass. This aerosol mass concentration ratio, which values were the highest during the pre-monsoon (0.39 ± 0.09) and lowest during winter (0.21 ± 0.05), is similar to those observed for arid sites (Shahsavani

et al., 2012; Lundgren et al., 1996), for sites affected both by dust storm originating in Asia (Claiborn et al., 2000) and strong African **dust outbreak episodes (Alastuey et al., 2005) and dusty roads** (Colbeck et al., 2011). Similar ratios were observed also in other large municipalities in South Asia, such as Bilaspur (0.24, Deshnukh et al., 2010) or Raipur (0.28, Deshmukh et al., 2013) in India, or Nanjing (0.34, Wang et al., 2003) in China. In the European cities this ratio is generally higher than in Asia.

3.3 SLCF/P behavior as a function of wind direction

We **highlighted** the wind sector which mostly contributed to the occurrence of high SLCF/P values at the measurement site, as presented in Fig. 5. Here, the angular distribution of the pollutants averaged over WD intervals of 10° (green lines) is shown. Also reported in the figure are the distributions of the frequency of wind directions (blue) and the relative abundance of the pollutants (red), weighted by the wind directions, computed according to Gilge et al. (2010). **These analyses refer to** the whole investigation period and no significant differences were observed by categorizing data as a function of the different seasons, nor time of day. WD behavior has already been presented in Sect. 3.1; BC and aerosol particle number (both accumulation and coarse) average values did not show any dependence as a function of wind direction: this is conceivable considering that Paknajol is located in the middle of several pollution sources. O_3 angular mean values (green line) showed enhanced values from W-NW sector (35 nmol/mol on average). This leads to a small distortion of the O_3 contribution away from the distribution of the wind directions (peaking at 270°) and 48% of the total O_3 recorded at Paknajol station was enclosed in the $240\text{-}320^\circ$ wind sector, which perfectly matches the direction from a mountain pass from where, according to Panday and Prinn (2009), air-masses can be transported during day-time towards Kathmandu due to thermal transport, indicating arrival of regional polluted air-masses.

3.4 Correlation analysis among SLCF/P

By looking at the diurnal variations presented in Fig. 3, the first peak in BC **and aerosol particles** can be explained in terms of increased emission (traffic and cooking activity) under atmospheric stable conditions and low PBL height or with an additional contribution of down-mixing as the night-time stable boundary layer breaks up (Panday and Prinn, 2009). Dilution within the higher PBL, arrival of cleaner air from west of the Kathmandu Valley, and decrease of emissions can explain the daily minimum in aerosol and BC observed from 11:00 to 17:00. Conversely, the peak in O_3 can be explained in terms of enhanced photochemical production (with respect to night-time or early morning), as well as downward vertical mixing of polluted regional air-masses from the

free troposphere or the night-time residual layer. When the PBL height starts to decline due to the diurnal decrease of solar radiation and soil heating, along with the increased emissions of the evening traffic and cooking activities, a secondary peak in BC aerosol is observed from 18:00 to 22:00. Titration with NO, dry deposition and less efficient vertical mixing within a more stable PBL lead to the decrease of O₃ which finally results in the night-time minimum, when BC and aerosol particles also present the lowest concentrations due to the decrease of traffic and domestic emissions. Moreover, since measurements were taking place on the roof of a tall building, in presence of a stable night-time atmosphere it may be difficult to capture near surface pollution. These behaviors led to a negative correlation between hourly BC and O₃ (Table 3), which was almost constant over all of the considered seasons. The O₃ decrease after the noon peak was faster during winter and post-monsoon seasons, while it was more gradual during pre-monsoon and monsoon. Moreover, during the pre-monsoon season, a “bump” in O₃ mixing ratios (>50 nmol/mol) was observed during the afternoon (between 11:00 and 17:00, Fig. 3). The simultaneous decreases of BC and aerosol particle concentrations support a strong role of downward vertical mixing in enhancing O₃ and decreasing primary pollutants (BC and aerosol particles). The important role of dynamics in influencing SLCF/P variability is confirmed by the negative (positive) correlation between wind speed and BC (O₃). The correlation coefficients (**r**) are higher by considering daily average values (Table 3), supporting the role of day-to-day meteorology in influencing the SLCF/P.

BC showed significantly higher hourly correlation with accumulation and coarse particles (0.86 and 0.87, respectively), which was lower during the wet season (0.66), strongly supporting common sources and processes influencing their variability (i.e. traffic sources and PBL dynamics). The lower correlation can be explained in terms of different hygroscopicity of BC with respect to other aerosol particles (see Marinoni et al., 2010), which can lead to lower scavenging efficiency of BC with respect to other inorganic and organic species that has been proved especially for not aged BC (Cozic et al., 2007). Due to the lack of data, no information about the variation of the correlation coefficients computed between accumulation and coarse particles could be given other than during pre-monsoon and monsoon seasons. The high correlation coefficient between BC and accumulation (and coarse) particle could however indicate that BC can be used as an indicator of **primary** pollution, even when measurements by the OPC are lacking.

O₃ showed high correlation with solar radiation (0.71 for hourly and 0.56 for daily values) and temperature, considered as a proxy for season (0.51 and 0.32): this is somewhat expected for an urban site like Kathmandu, where photochemistry and PBL dynamics (indirectly driven by solar radiation and temperature behavior) play an important role in determining O₃ variability (Pudasainee et al., 2006). The correlation with solar radiation exhibited some variability during the

year, giving the lowest values (0.59 for hourly and 0.06 for daily values) during the pre-monsoon season, possibly supporting the enhanced role of atmospheric transport and dynamics in influencing O₃ with respect to photochemistry. Apparently, this agrees only in part with the results shown in Pudasainee et al. (2006), in which the authors argued that the “flat peak” in O₃ concentrations during the pre-monsoon is mainly due to abundance of solar radiation and higher temperature (justified by high correlation coefficient values).

In order to distinguish the chemical effects from the boundary layer dynamics, we also computed correlation coefficients limiting the data to convective hours only (i.e. between 11:00 and 17:00, according to the wind speed and solar radiation diurnal variations). The slight weaker correlation between BC and accumulation particle number and, on the other hand, the increase in correlation between O₃ and accumulation particle number may indicate the role of other processes (e.g. secondary aerosol production) occurring in the air-masses which characterize this specific time span (Table S1, Supplement). In particular, we suppose that aged air-masses rich in secondary pollutants (i.e. O₃ and aerosol) can be transported to the measurement site in the afternoon mixed layer.

Here, we argue that mixing processes with upper residual O₃ layers can explain this behavior. Sensitivity tests with a recurrent neural network model, using different subgroups of proxies, have been carried out and the results are shown in Fig. 6, where the observed and different simulated average diurnal O₃ mixing ratios are compared. The simulation that included all the proxies reproduced quite well the observed O₃ mixing ratios for all hours of the day, whereas a simulation that included only wind speed (a good proxy of atmospheric dynamics) reproduced with accuracy the afternoon (after 15:00) and evening levels of O₃, missing completely the main O₃ peak before noon. In contrast, by using as input parameters both wind speed and solar radiation, the model reproduced well the peak before noon and the high levels of afternoon-evening O₃. Putting together the results of these two simulations, we can conclude that the high level of O₃ during the afternoon is mainly due to dynamics (vertical intrusion from upper atmospheric layers and/or horizontal advection), for the following two reasons: (i) in the model, the wind speed used as input is enough to reproduce the afternoon concentrations of O₃ and (ii) the inclusion of solar radiation does not improve the agreement between measured and modelled O₃ during the afternoon, but substantially enhances the agreement between measurements and simulations before noon, when photochemistry, as expected, plays a larger role. The photochemistry contribution varied as a function of the hour of the day, ranging from 6% to 34%.

3.5 Influence of atmospheric synoptic circulation

3.5.1 Synoptic-scale air-mass circulation scenarios

With the purpose of investigating the variability of large-scale atmospheric circulation affecting the region of interest, we clustered the HYSPLIT 5-days back-trajectories. Here, it should be clearly stated that this analysis has been carried out with the aim of providing information about the synoptic-scale circulation scenarios which affect the region where the Kathmandu Valley is located and therefore investigating the link among these scenarios with the SLCF/P variability. In order to retain robust information, only the days for which the same cluster was observed for at least $\frac{3}{4}$ of daily observations were considered in this analysis. Overall, 9 clusters were identified; Figure 7 shows the percentage of occurrence for each cluster for the whole investigation period, as a function of the different seasons. 3 clusters out of 9 had a very small percentage of occurrences (i.e. less than 5% of air-masses for each of these clusters were recorded), thus were not retained for further analysis (see Supplementary Material). “Regional” (REG, 21.9%) and “Western” (WES, 21.4%) clusters showed the highest occurrence values. The first encompasses trajectories within a $10^{\circ} \times 10^{\circ}$ area centered on the region of interest, thus indicating the occurrence of regional-scale atmospheric circulation: trajectories from this area were present in every season, except winter. WES, on the other hand, represents westerly air-masses which originated (5-days backward in time) at a longitude around 60° E. The cyclonic behavior of these back-trajectories indicated that synoptic-scale westerly disturbances could steer air-masses under these scenarios. A significant fraction of trajectories (16.3%), mostly observed during pre-monsoon and winter, showed again westerly transport at synoptic-scale (even if presenting higher horizontal velocities with respect to WES): 5-day back-trajectories originated or travelled over desert areas of Arabian Peninsula (ARAB-PEN). The larger latitudinal span of these back-trajectories suggested that synoptic-scale disturbances and subtropical jet stream latitudinal excursions could steer the air-masses towards the region of interest. During the monsoon and post-monsoon seasons, the atmospheric circulation was strongly affected by the summer monsoon and by the occurrence of low pressure areas in the Bay of Bengal, which enhanced the possibility to observe easterly circulation: i.e. “Bay of Bengal” (BENG, 12.8%) and “Eastern” (EAS, 14.8%) clusters. Finally, a not negligible fraction of days (5.6%, occurring mostly during winter) can be tagged to south-westerly circulation (SW), which can be related to the passage of synoptic-scale disturbances over the western Indian subcontinent (Böhner, 2006). For more details and plots concerning the different back-trajectory clusters, please see the Supplementary Material.

3.5.2 Influence of atmospheric circulation on O₃ and BC diurnal variations

The BC and O₃ diurnal variations, as a function of the different synoptic-scale air-mass circulation scenarios (Sect. 3.5.1) are shown in Fig. 8. The BC diurnal variation was only partly

dependent from the air-mass clusters: the shape was the same for all of the clusters, although a difference in the amplitude of the cycles was recorded. In particular, regional air-masses or on the eastern regions (BENG and EAS) were associated to smaller BC values both during peaks and minimum levels. This is because air-masses from these regions were retrieved only during monsoon and post-monsoon seasons, when BC concentrations were at their minimum (no occurrences at all were registered during winter) due to enhanced wash-out. On the other hand, during winter and pre-monsoon, the highest values of BC were recorded under ARAB-PEN, WES and SW air-mass circulation. Particularly, the diurnal cycle of BC and the relative 24-hour averaged peak values in the morning and in the evening were maximized when SW circulation affected the measurement site.

Concerning O₃ diurnal variation, significant differences can be observed as a function of different synoptic-scale circulation scenarios. Despite a moderate diurnal cycle of BC, the highest diurnal peak value and the largest amplitude of daily cycle were observed for the WES circulation: we can hypothesize that air-masses from the free troposphere or overpassing polluted regions above the Indo-Gangetic Plain could contribute in the appearance of these high values. It is interesting to note that for the three synoptic scale scenarios, most frequent during pre-monsoon and winter (i.e. WES, ARAB-PEN and SW), very different results were obtained for BC and O₃. In particular, the diurnal peaks were maximized (minimized) for O₃ (BC). This can be tentatively explained by suggesting that, under this circulation, meteorological conditions should favor the dilution of polluted air-masses emitted from surface sources and transport of O₃-rich upper layers by vertical entrainment processes (e.g. Kleinman et al., 1994). Similar diurnal cycles but lower mixing ratios were tagged to ARAB-PEN and REG circulations. As for BC, the smallest O₃ diurnal cycles were linked to the typical monsoon circulations EAS and BENG: this is in agreement with Agrawal et al. (2008) who indicated that, due to widespread rain precipitation and cloudy conditions, summer monsoon is not favorable to photochemical O₃ production and to the occurrence of elevated O₃ regime. With respect to other atmospheric circulation, the average O₃ diurnal cycles for ARAB-PEN, REG and WES were characterized by high values from 13:00 to 21:00, while an intermediate condition was observed for the SW circulation.

3.6 Influence of open vegetation fires on BC and O₃ values

As shown in Putero et al. (2014), the BC and O₃ values in Nepal are partly influenced by the emissions from open vegetation fires, occurring across broad regions. In order to evaluate the contribution of large open fires emissions to the BC and O₃ variations observed at Paknajol, the daily total number of fires by the MODIS product has been retrieved and used. Fire pixels (with a

confidence value $\geq 75\%$) were derived from the MODIS Global Monthly Fire Location Product (MCD14ML); these have been “filtered” by means of the MODIS Land Cover Climate Modeling Grid Product (MCD12C1), in order to retain only fires occurring over specific land use categories (i.e. vegetation, croplands, forests; for more details on such products, see Justice et al., 2002; Friedl et al., 2010). This methodology did not allow us to account for the fraction that came from “residential” burning (e.g. garbage burning occurring in urban areas, or domestic). The study area for the open vegetation fires occurrences was the Southern Himalayas box ($26^\circ \text{ N} \leq \text{Lat} \leq 30^\circ \text{ N}$; $80^\circ \text{ E} \leq \text{Lon} \leq 88^\circ \text{ E}$) considered in Putero et al. (2014) as the main contributor for Nepal. Over the whole period, the correlation coefficient between the number of fires and the delayed (from t to $t-3$ days) BC concentrations showed almost null correlation (0.10), pointing out that, in general, the BC fraction could be mainly influenced by other (local) anthropogenic emissions, also including the contribution from domestic and garbage burning. A sensitivity study was carried out by considering slightly different spatial domains for the fire detection, without significant changes of the results. Nevertheless, some BC peaks have been superimposed to periods of high fire activities. During these events, the large-scale synoptic scenario, as deduced by HYSPLIT, showed WES and REG circulation, thus supporting the presence of regional-scale transport, and the possible influence from specific distinct (major) events of open vegetation fires. However, several limitations of the use of back-trajectories and MODIS data (which can miss short-time events, small fires, and fires under clouds) have to be taken into account; for this reason, the use of chemical transport modeling outputs would be required for investigating these events in deeper detail. Figure 9 shows the diurnal BC and O_3 variations for the period of study (panels *a-b*) and the time series of total daily fires over the Southern Himalayas box (as defined above) retrieved by MODIS (panel *c*).

BC diurnal variation seemed to remain pretty constant over the entire time period, thus suggesting no prominent influence by fire emissions. During high fire activity periods (e.g. during the pre-monsoon season), BC showed increased concentrations, even though no shift of the daily maxima position occurred, thus indicating that local emissions (traffic and/or domestic, including open garbage burning) and PBL dynamic are the main factors influencing BC concentrations at Paknajol, further supported by the high ratio BC/PM_{10} . The same could not be said considering O_3 measurements. When the number of fires was at the highest values, the O_3 peak was “shifted” in time and appeared in the late afternoon (between 16:00 and 18:00). This period almost perfectly matched with the “bump” in O_3 observed at diurnal scale during the pre-monsoon season (Sect. 3.4). Here we hypothesize that biomass burning plumes that were enriched in O_3 photochemically produced after enhanced emission of precursors (e.g. CO, VOCs) could be transported over

Kathmandu and possibly mixed within PBL due to efficient vertical mixing between upper ozone layers and surface layer.

4. Conclusions

In this work, we analyzed one full year of hourly-resolution data (February 2013 – January 2014) of SLCF/P (BC and O₃) as well as aerosol number and mass concentration, observed at Paknajol, an urban site in central Kathmandu city, Nepal. Very high values of SLCF/P were detected during the whole measurement period, indicating persistent poor air quality conditions, dangerous for the human health and the environment, including influence on local/regional climate.

Equivalent BC, aerosol number concentration and mass presented seasonal cycles with the highest values during winter and pre-monsoon and minima during the summer. Surface O₃ was characterized by maximum values during the pre-monsoon and a diurnal cycle (day-time maxima) **opposite to what was observed** for aerosol (mid-day minimum and maximum early in the morning and late evening). The diurnal behavior of BC and aerosol number concentration indicated that local pollution sources, mostly related to road traffic or domestic emissions, represent the major contribution to air pollution in Kathmandu.

Concerning O₃, **the analysis of the seasonal change of the diurnal cycle** and correlation with meteorological parameters and aerosol properties suggested that, apart from photochemistry (**which contribution ranges from 6% to 34%**), PBL dynamics and wind circulation have a significant role in determining its variability: during mid-day, air-masses richer in O₃ appeared to be transported to the measurement site by flows through the mountain passes located at the western rim of the Kathmandu valley. Especially during pre-monsoon, high O₃ values were observed during the afternoon. We suggest that mixing and vertical entrainment processes between upper layers and PBL could partially explain the occurrence of these high values and can lead to favorable conditions for O₃ production that will often result in exceedance of guideline values set by the World Health Organization (WHO).

The possible impact of emissions by major open vegetation fires occurring at regional scale has been assessed by analyzing MODIS fire distribution: a significant impact has been observed only for O₃ and during specific episodes, able to affect day-to-day variability. Despite the limitations of the methodology (e.g. garbage and domestic burning were not considered in this analysis and small or short-lasting open fires can be missed by satellite detection), this indicates that the occurrence of widespread biomass burning emissions can represent, in particular during the pre-monsoon season, a not-negligible source of precursors for O₃ photochemical production in the Kathmandu Valley.

The analysis of large-scale atmospheric circulation demonstrated a significant impact of the “background” synoptic-scale circulation on diurnal cycles of BC and O₃ in Kathmandu. In particular, atmospheric circulation related to westerly (WES, ARAB-PEN, SW) and regional (REG) circulations appeared to be especially conducive for the occurrence of the high BC and O₃ values.

Considering the 24 h limit of 120 µg/m³ proposed for PM₁₀ measurements from Government of Nepal (Giri et al., 2006), we found, for the 2013 period, a total of 124 exceedances, 51.4% of the available PM₁₀ data. In 2003, the Nepali Ministry of Population and Environment (MoPE) has also defined five different quality descriptions (classes) based on PM₁₀ levels (see HMG/MOPE, 2003). During our observation period, following these references, 12 days (5% of data) were categorized as “Good” (range 0-60 µg/m³), 105 as “Moderate” (61-120 µg/m³) and 103 days were tagged as “Unhealthy” (121-350 µg/m³), representing 43.6% and 42.7% of data, respectively. A total of 21 days (8.7%) were classified as “Very Unhealthy” (351-425 µg/m³, 13 days) or “Hazardous” (>425 µg/m³, 8 days). Therefore, these data reveal the poor air quality in Kathmandu, also considering that the WHO guideline defines the limits of 20 µg/m³ per year and 50 µg/m³ per 24 hour. WHO (2006) also defined air quality **guidelines for O₃ based** on the analysis of the daily maximum 8-hour concentrations: High Levels (HL: 240 µg/m³); Interim Target-1 (IT-1: 160 µg/m³) and Air Quality Guideline (AQG: 100 µg/m³). Based on Paknajol data, we found 13 days exceeding the IT-1 (3.5% of the data-set) and 125 days (34% of the data-set) exceeding the AQG. It should be noted that WHO associated “important health effects” to IT-1 exceedances, indicating that the exposures at the IT-1 level increases the number of attributable deaths by 3–5%. On the other side, the exceedances of the AQG are related to an estimated 1–2% increase in daily mortality (WHO, 2006). The totality of IT-1 exceedances were recorded during the pre-monsoon season, while AQG exceedances were observed for 62% during the pre-monsoon, 22% during the monsoon and the remaining during post-monsoon (4%) and winter (12%). Roughly, the total number (97%) of exceedances (IT-1 and AQG) were observed from 10:00 to 18:00. It is worth noting that 37 days (all detected during the pre-monsoon) were affected by the occurrence of major open vegetation fire activity during the investigated period. By neglecting these days, all of the IT-1 exceedances for O₃ at Paknajol were removed, and 88 AQG exceedances were retained (all the days with fire activity were tagged to AQG exceedances), representing a 29% (47%) decrease on a yearly (seasonal) basis.

The information of this study, developed in the framework of the SusKat-ABC project, may be useful for implementing control measures to mitigate the occurrence of acute pollution levels in the Kathmandu municipality, as well as for improving regional climate conditions, important for the wide area that lies at the foothills of the pristine Himalayan environment.

Acknowledgments

This work was supported by the National Project NextData, funded by the Italian Ministry of University and Research. The authors thank the Institute for Advanced Sustainability Studies (IASS) and the International Centre for Integrated Mountain Development (ICIMOD) that led the Sustainable Atmosphere for the Kathmandu Valley (SusKat) project. This study was partially supported by core funds of ICIMOD contributed by the governments of Afghanistan, Australia, Austria, Bangladesh, Bhutan, China, India, Myanmar, Nepal, Norway, Pakistan, Switzerland, and the United Kingdom. The usual disclaimers apply.

References

- Agrawal, M, Auffhammer, M, Chopra, U K, Emberson, L, Iyengararasan, M, Kalra, N, Ramana, M V, Ramanathan, V, Singh, A K, and Vincent, J, 2008. Impacts of Atmospheric Brown Clouds on agriculture, Part II of Atmospheric Brown Clouds: regional assessment report with focus on Asia, Project Atmospheric Brown Cloud, UNEP, Nairobi, Kenya.
- Alastuey, A, Querol, X, Castillo, S, Escudero, M, Avila, A, Cuevas, E, Torres, C, Romero, P-M, Exposito, F, Garcia, O, Diaz, J P, Van Dingenen, R, and Putaud, J P, 2005. Characterisation of TSP and PM_{2.5} at Izaña and Sta. Cruz de Tenerife (Canary Islands, Spain) during a Saharan Dust Episode (July 2002). *Atmospheric Environment* 39, 4715-4728.
- Aryal, R K, Lee, B-K, Karki, R, Gurung, A, Kandasamy, J, Pathak, B K, Sharma, S, and Giri, N, 2008. Seasonal PM₁₀ dynamics in Kathmandu valley. *Atmospheric Environment* 42, 8623-8633.
- Biancofiore, F, Verdecchia, M, Di Carlo, P, Tomassetti, B, Aruffo, E, Busilacchio, M, Bianco, S, Di Tommaso, S, and Colangeli, C, 2015. Analysis of surface ozone using a recurrent neural network, *Science of the Total Environment* 514, 379–387.
- Böhner, J, 2006. General climatic controls and topoclimatic variations in Central and High Asia. *BOREAS* 35, 279-294.
- Bonasoni, P, Laj, P, Marinoni, A, Sprenger, M, Angelini, F, Arduini, J, Bonafè, U, Calzolari, F, Colombo, T, Decesari, S, Di Biagio, C, di Sarra, A G, Evangelisti, F, Duchi, R, Facchini, MC, Fuzzi, S, Gobbi, G P, Maione, M, Panday, A, Roccatò, F, Sellegri, K, Venzac, H, Verza, GP, Villani, P, Vuillermoz, E, and Cristofanelli, P, 2010. Atmospheric Brown Clouds in the Himalayas: first two years of continuous observations at the Nepal Climate Observatory-Pyramid (5079 m). *Atmospheric Chemistry and Physics* 10, 7515-7531.
- Chevalier, A, Gheusi, F, Delmas, R, Ordonez, C, Sarrat, C, Zbinden, R, Thouret, V, Athier, G, and Cousin, J-M, 2007. Influence of altitude on ozone levels and variability in the lower

- troposphere: a ground-based study for western Europe over the period 2001-2004. *Atmospheric Chemistry and Physics* 7, 4311-4326.
- Claiborn, C S, Finn, D, Larson, T V, and Koenig, J Q, 2000. Windblown dust contributes to high PM_{2.5} concentrations. *Journal of the Air & Waste Management Association*, 50 (8), 1440-1445.
- Colbeck, I, Nasir, Z A, Ahmad, S, and Ali, Z, 2011. Exposure to PM₁₀, PM_{2.5}, PM₁ and Carbon Monoxide on roads in Lahore, Pakistan. *Aerosol Air Quality Research* 11, 689-695.
- Cozic, J, Verheggen, B, Mertes, S, Connolly, P, Bower, K, Petzold, A, Baltensperger, U, and Weingartner, E, 2007. Scavenging of black carbon in mixed phase clouds at the high alpine site Jungfraujoeh. *Atmospheric Chemistry and Physics* 7, 1797-1807.
- Cristofanelli, P, Bracci, A, Sprenger, M, Marinoni, A, Bonafè, U, Calzolari, F, Duchi, R, Laj, P, Pichon, JM, Roccatò, F, Venzac, H, Vuillermoz, E and Bonasoni, P, 2010. Tropospheric ozone variations at the Nepal Climate Observatory-Pyramid (Himalayas, 5079 m a.s.l.) and influence of deep stratospheric intrusion events. *Atmospheric Chemistry and Physics* 10, 6537-6549.
- Deshmukh, D K, Deb, M K, and Verma, S K, 2010. Distribution patterns of coarse, fine and ultrafine atmospheric aerosol particulate matters in major cities of Chhattisgarh. *Indian Journal of Environmental Protection* 30, 184-197.
- Deshmukh, D K, Deb, M K, and Mkoma, S L, 2013. Size distribution and seasonal variation of size-segregated particulate matter in the ambient air of Raipur city, India. *Air Quality, Atmosphere and Health* 6, 259-276.
- Di Carlo, P, Pitari, G, Mancini, E, Gentile, S, Pichelli, E, and Visconti, G, 2007. Evolution of surface ozone in central Italy based on observations and statistical model. *Journal of Geophysical Research* 112, D10316, doi: 10.1029/2006JD007900.
- Draxler, R. R., and Hess, G. D., 1998. An overview of the HYSPLIT_4 modelling system for trajectories, dispersion and deposition. *Australian Meteorological Magazine* 47, 295-308.
- Draxler, R. R., 1999. HYSPLIT4 user's guide. NOAA Tech. Memo. ERL ARL-230, NOAA Air Resources Laboratory, Silver Spring, MD.
- Elman, L J, 1990. Finding structure in time. *Cognitive Science* 14, 179-211.
- Faiz, A, Ale, B B, and Nagarkoti, R K, 2006. The role of inspection and maintenance in controlling vehicular emissions in Kathmandu Valley, Nepal. *Atmospheric Environment* 40, 5967-5975.
- Friedl, M A, Sulla-Menashe, D, Tan, B, Schneider, A, Ramankutty, N, Sibley, A, and Huang, X, 2010. MODIS Collection 5 global land cover: algorithm refinements and characterization of new datasets. *Remote Sensing Environment*, 114, 168-182.

- Gilge, S, Plass-Duelmer, C, Fricke, W, Kaiser, A, Ries, L, Buchmann, B, and Steinbacher, M, 2010. Ozone, carbon monoxide and nitrogen oxides time series at four alpine GAW mountain stations in central Europe. *Atmospheric Chemistry and Physics* 10, 12295-12316.
- Giri, D, Murthy, K, Adhikary, P R, and Khanal, S N, 2006. Ambient air quality of Kathmandu valley as reflected by atmospheric particulate matter concentrations (PM₁₀). *International Journal of Environmental Science and Technology* 3 (4), 403-410.
- HMG/MOPE, 2003. Draft report on air emission inventory. Kathmandu, Nepal.
- Hyvärinen, A-P, Vakkari, V, Laakso, L, Hooda, R K, Sharma, V P, Panwar, T S, Beukes, J P, van Zyl, P G, Josipovic, M, Garland, R M, Andreae, M O, Pöschl, U, and Petzold, A, 2013. Correction for a measurement artifact of the Multi-Angle Absorption Photometer (MAAP) at high black carbon mass concentration levels. *Atmospheric Measurement Techniques* 6, 81-90.
- India Meteorological Department (IMD), 2014. Monsoon report 2013. Edited by Pai, D S, and Bhan S C. Pune, India.
- Jacobson, M Z, 2002. *Atmospheric pollution: history, science and regulation*. Cambridge University Press, Cambridge, United Kingdom and New York, NY, USA.
- Justice, C O, Giglio, L, Korontzi, S, Owens, J, Morisette, J T, Roy, D, Descloitres, J, Alleaume, S, Petitcolin, F, and Kaufman, Y, 2002. The MODIS fire products. *Remote Sensing Environment*, 83, 244-262.
- Klausen, J, Zellweger, C, Buchmann, B, and Hofer, P, 2003. Uncertainty and bias of surface ozone measurements at selected Global Atmosphere Watch sites. *Journal of Geophysical Research* 108 (D19), 4622, doi:10.1029/2003JD003710.
- Kleinman, L, Lee, Y-N, Springston, S R, Nunnermacker, L, Zhou, X, Brown, R, Hallock, K, Klotz, P, Leahy, D, Lee, J H, and Newman, L, 1994. Ozone formation at a rural site in the southeastern United States. *Journal of Geophysical Research*, 99 (D2), 3469-3482.
- Lönnblad, L, Peterson, C, Röngvalsson, T, 1992. Pattern recognition in high energy physics with artificial neural network — Jetnet 2.0. *Computer Physics Communications* 70, 167–182.
- Lundgren, D A, Hlaing, D N, Rich, T A, and Marple, V A, 1996. PM₁₀/PM_{2.5}/PM₁ data from a trichotomous sampler. *Aerosol Science and Technology* 25 (3), 353-357.
- Marinoni, A, Cristofanelli, P, Laj, P, Duchi, R, Calzolari, F, Decesari, S, Sellegri, K, Vuillermoz, E, Verza, GP, Villani, P and Bonasoni, P, 2010. Aerosol mass and black carbon concentrations, a two year record at NCO-P (5079 m, Southern Himalayas). *Atmospheric Chemistry and Physics* 10, 8551-8562.

- Monks, P S, Granier, C, Fuzzi, S, Stohl, A, Williams, M L, Akimoto, H, Amann, M, Baklanov, A, Baltensperger, U, Bey, I, Blake, N, Blake R S, Carslaw, K, Cooper O R, Dentener, F, Fowler, D, Fragkou, E, Frost, G J, Generoso, S, Ginoux, P, Grewe, V, Guenther, A, Hansson, H C, Henne, S, Hjorth, J, Hofzumahaus, A, Huntrieser, H, Isaksen, I S A, Jenkin, M E, Kaiser, J, Kanakidou, M, Klimont, Z, Kulmala, M, Lawrence, M G, Lee, J D, Liousse, C, Maione, M, and McFiggans, G, 2009. Atmospheric composition change – global and regional air quality. *Atmospheric Environment* 43, 5268-5350.
- Panday, A, and Prinn, R G, 2009. Diurnal cycle of air pollution in the Kathmandu Valley, Nepal: Observations. *Journal of Geophysical Research*, 114, D09305, doi:10.1029/2008JD009777.
- Panday, A, Prinn, R G, and Schär, C, 2009. Diurnal cycle of air pollution in the Kathmandu Valley, Nepal: 2. Modeling results. *Journal of Geophysical Research*, 114, D21308, doi: 10.1029/2008JD009808.
- Pudasainee D, Balkrishna S, Shrestha, M L, Kaga, A, Kondo, A, and Inoue, Y, 2006. Ground level ozone concentrations and its association with NO_x and meteorological parameters in Kathmandu valley, Nepal. *Atmospheric Environment* 40, 8081-8087.
- Putero, D, Landi, T C, Cristofanelli, P, Marinoni, A, Laj, P, Duchi, R, Calzolari, F, Verza, G P, and Bonasoni, P, 2014. Influence of open vegetation fires on black carbon and ozone variability in the southern Himalayas (NCO-P, 5079 m a.s.l.). *Environmental Pollution* 184, 597-604.
- Ramanathan, V., Li, F., Ramana, M. V., Praveen, P. S., Kim, D., Corrigan, C. E., Nguyen, H., Stone, E. A., Schauer, J. J., Carmichael, G. R., Adhikary, B., and Yoon, S. C., 2007. Atmospheric brown clouds: Hemispherical and regional variations in long-range transport, absorption, and radiative forcing. *Journal of Geophysical Research* 112, D22S21, doi: 10.1029/2006JD008124.
- Ramanathan, V., and Carmichael, G., 2008. Global and regional climate changes due to black carbon. *Nature Geoscience* 1, 221-227.
- Rupakheti, M, Panday, A K, Lawrence, M G, Kim, S W, Sinha, V, Kang, S C, Naja, M, Park, J S, Hoor, P, Holben, B, Bonasoni, P, Sharma, R K, Mues, A, Mahata, K, Bhardwaj, P, Sarkar, C, Rupakheti, D, Regmi, R P, and Gustafsson, Ö, 2015. Air pollution in the Himalayan foothills: Overview of the SusKat-ABC international air pollution measurement campaign in Nepal. To be submitted to *Atmospheric Chemistry and Physics*.
- Shahsavani, A, Naddafi, K, Jafarzade Haghighifard N, Mesdaghinia, A, Yunesian, M, Nabizadeh, R, Arahani, M, Sowlat, M H, Yarahmadi, M, Saki, H, Alimohamadi, M, Nazmara, S, Motevalian, S A, and Goudarzi, G, 2012. The evaluation of PM₁₀, PM_{2.5} and PM₁

concentrations during the Middle Eastern Dust (MED) events in Ahvaz, Iran, from april through September 2010. *Journal of Arid Environments* 77, 72-83.

Sharma, C K, 1997. Urban air quality of Kathmandu Valley “Kingdom of Nepal”. *Atmospheric Environment* 31 (17), 2877-2883.

Sharma, R K, Bhattarai, B K, Sapkota, B K, Gewali, M B, and Kjeldstad, B, 2012. Black carbon aerosols variation in Kathmandu valley, Nepal. *Atmospheric Environment* 63, 282-288.

Shindell, D, Kuylenstierna, J C I, Vignati, E, van Dingenen, R, Amann, M, Klimont, Z, Anenberg, S C, Muller, N, Janssens-Maenhout, G, Raes, F, Schwartz, J, Faluvegi, G, Pozzoli, L, Kupiainen, K, Höglund-Isaksson, L, Emberson, L, Streets, D, Ramanathan, V, Hicks, K, Kim Oanh, N T, Milly, G, Williams, M, Demkine, V, and Fowler, D, 2012. Simultaneously mitigating near-term climate change and improving human health and food security. *Science* 335, 183-189.

Shrestha, P, Barros, A P, and Khlystov, A, 2010. Chemical composition and aerosol size distribution of the middle mountain range in the Nepal Himalayas during the 2009 pre-monsoon season. *Atmospheric Chemistry and Physics* 10 (23), 11605-11621.

Shrestha, R M and Malla, S, 1996. Air pollution from energy use in a developing country city: the case of Kathmandu Valley, Nepal. *Energy* 21 (9), 785-794.

Shrestha, R M, and Rajbhandari, S, 2010. Energy and environmental implications of carbon emission reduction targets: Case of Kathmandu Valley, Nepal. *Energy Policy* 38 (9), 4818-4827.

Shrestha, S R, Kim Oanh, N T, Xu, Q, Rupakheti, M, and Lawrence, M G, 2013. Analysis of the vehicle fleet in the Kathmandu Valley for estimation of environment and climate co-benefits of technology intrusions. *Atmospheric Environment* 81, 579-590.

UNEP and WMO, 2011. *Integrated Assessment of Black Carbon and Tropospheric Ozone*. UNEP, Nairobi.

Wang, G, Wang, H, Yu, Y, Gao, S, Feng, J, Gao, S, and Wang, L, 2003. Chemical characterization of water-soluble components of PM₁₀ and PM_{2.5} atmospheric aerosols in five locations of Nanjing, China. *Atmospheric Environment* 37, 2893-2902.

World Health Organization, 2006: *WHO Air quality guidelines for particulate matter, ozone, nitrogen dioxide and sulfur dioxide, Global update 2005, Summary of risk assessment*. WHO Press, Geneva, Switzerland.

Table 1. Onset and decay dates of the different seasons selected in this work.

Season	Start day – End day
Pre-monsoon	1 February – 12 May 2013
Monsoon	13 May – 6 October 2013
Post-monsoon	7 October – 26 October 2013
Winter	27 October 2013 – 31 January 2014

Table 2. Average values (\pm standard deviation) of the pollutants, computed for the different seasons selected by the periods of Table 1.

	O ₃ (nmol/mol)	BC ($\mu\text{g}/\text{m}^3$)	Accum. ($\#/\text{cm}^3$)	Coarse ($\#/\text{cm}^3$)	PM ₁ ($\mu\text{g}/\text{m}^3$)	PM ₁₀ ($\mu\text{g}/\text{m}^3$)
Pre-monsoon	38.0 \pm 25.6	14.5 \pm 10.4	668 \pm 383	4.2 \pm 2.5	98 \pm 83	241 \pm 134
Monsoon	24.9 \pm 16.5	6.3 \pm 3.8	250 \pm 141	1.9 \pm 1.1	32 \pm 12	107 \pm 37
Post-monsoon	22.8 \pm 17.0	6.2 \pm 3.9	-	-	26 \pm 10	101 \pm 38
Winter	20.0 \pm 19.8	18.3 \pm 14.1	-	-	74 \pm 26	320 \pm 75
All	27.0 \pm 21.3	11.6 \pm 10.7	505 \pm 372	3.3 \pm 2.4	48 \pm 42	169 \pm 113

Table 3. Correlation coefficients (r) between several parameters (BC, O₃, accumulation and coarse particles, WS, T and RAD) for hourly and daily (in parentheses) values, over the whole sampling period.

	O ₃	BC	Acc.	Coarse	WS	T	RAD
O ₃	-	-0.21 (-0.04)	0.11 (0.43)	0.07 (0.41)	0.54 (0.65)	0.51 (0.32)	0.71 (0.56)
BC	-0.21 (-0.04)	-	0.86 (0.78)	0.87 (0.74)	-0.35 (-0.21)	-0.56 (-0.58)	-0.10 (-0.15)
Acc.	0.11 (0.43)	0.86 (0.78)	-	0.86 (0.91)	-0.22 (0.12)	-0.39 (-0.38)	-0.02 (-0.06)
Coarse	0.07 (0.41)	0.87 (0.74)	0.86 (0.91)	-	-0.21 (0.18)	-0.31 (-0.35)	-0.07 (-0.03)
WS	0.54 (0.65)	-0.35 (-0.21)	-0.22 (0.12)	-0.21 (0.18)	-	0.45 (0.41)	0.40 (0.56)
T	0.51 (0.32)	-0.56 (-0.78)	-0.39 (-0.38)	-0.31 (-0.35)	0.45 (0.41)	-	0.43 (0.31)
RAD	0.71 (0.56)	-0.10 (-0.15)	-0.02 (-0.06)	-0.01 (-0.03)	0.40 (0.56)	0.43 (0.31)	-

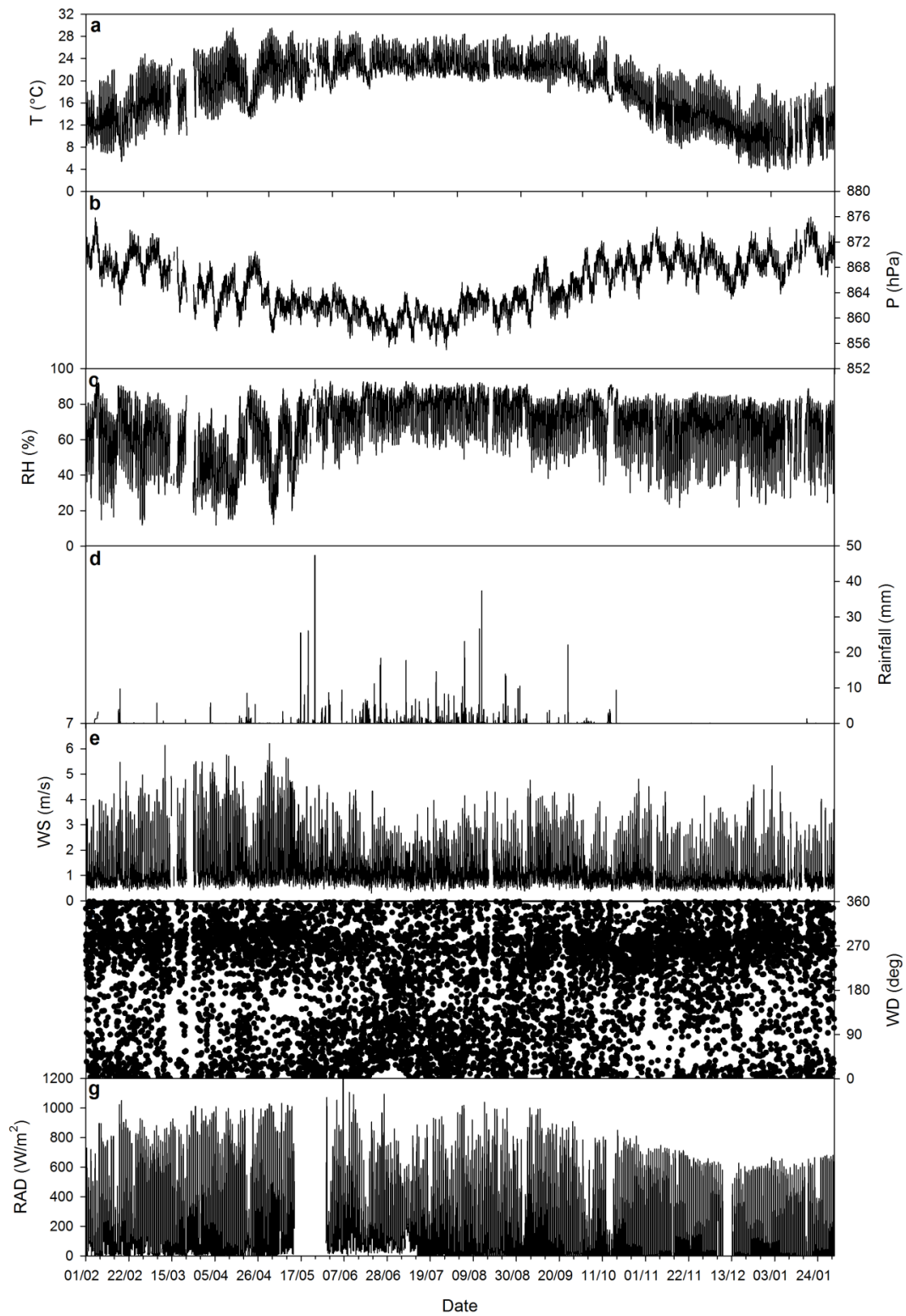


Figure 1. Time series of hourly atmospheric temperature (T, panel *a*), pressure (P, panel *b*), relative humidity (RH, panel *c*), precipitation (*d*), wind speed (WS, panel *e*), wind direction (WD, panel *f*) and solar radiation (RAD, panel *g*) measured at Paknajok.

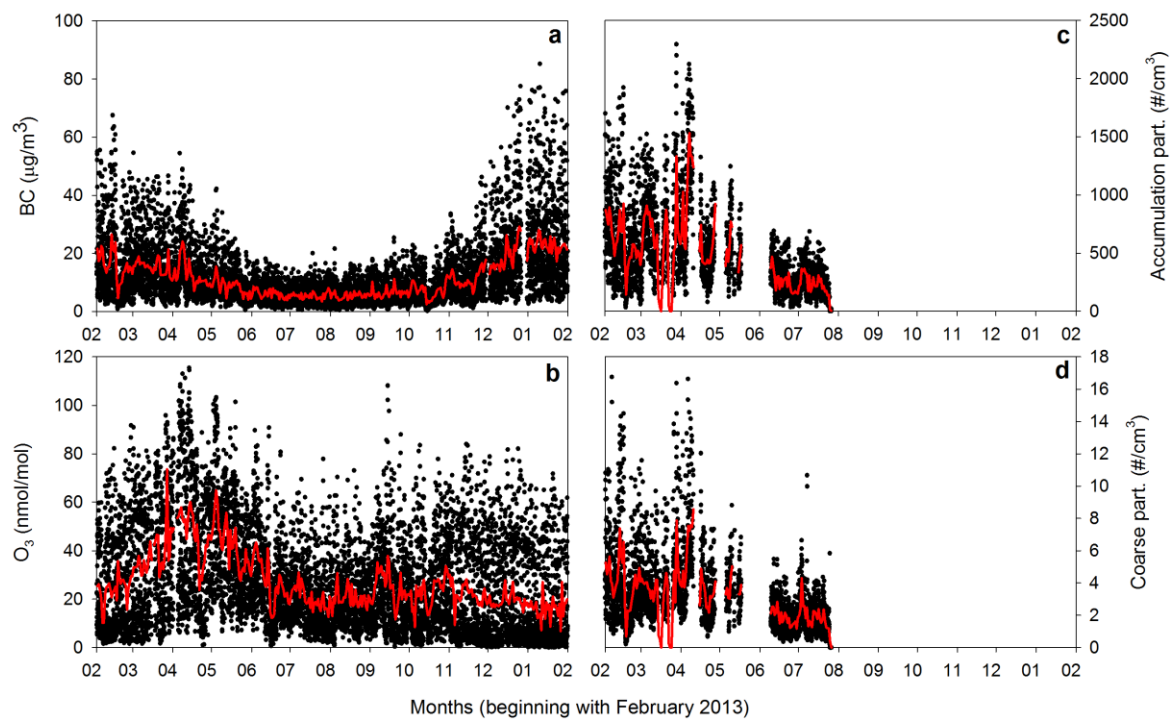


Figure 2. Time series of hourly concentrations of equivalent black carbon (panel *a*), surface ozone (*b*), accumulation (*c*) and coarse particles (*d*) recorded at Paknajol. Red lines denote daily averages.

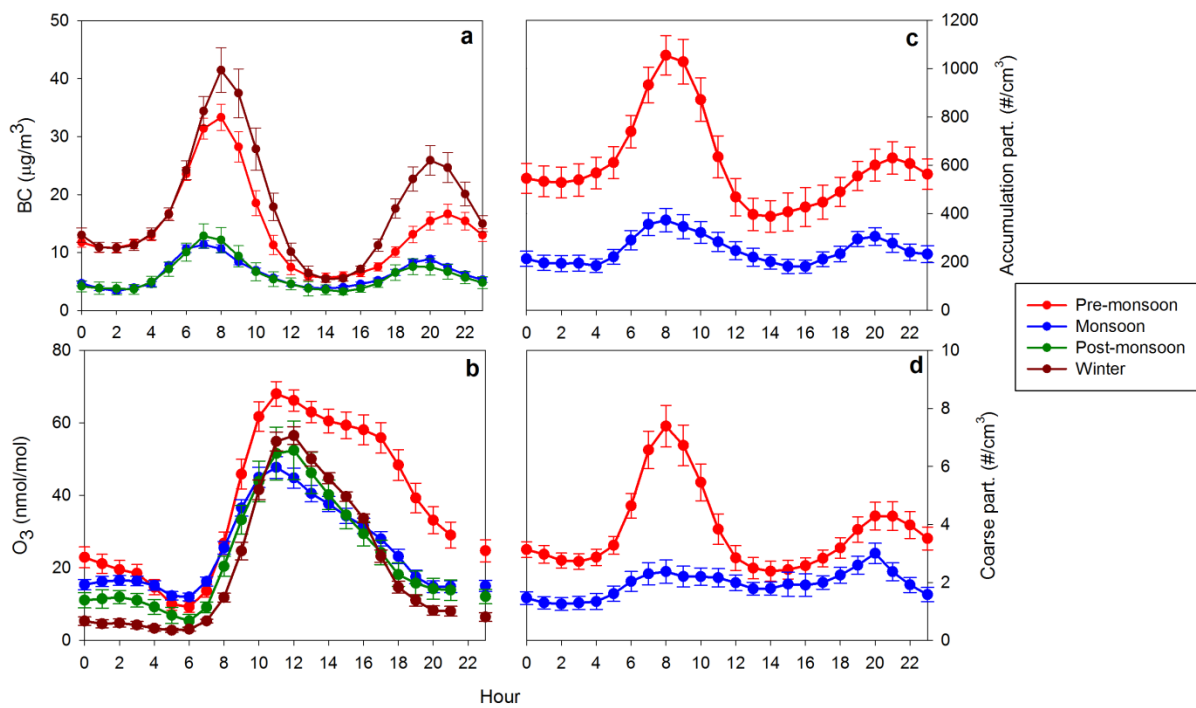


Figure 3. Average seasonal diurnal variation for equivalent black carbon (panel *a*), surface ozone (b), accumulation (c) and coarse (d) particles collected at Paknajol. The error bars denote the expanded uncertainties ($p < 0.05$) of the mean.

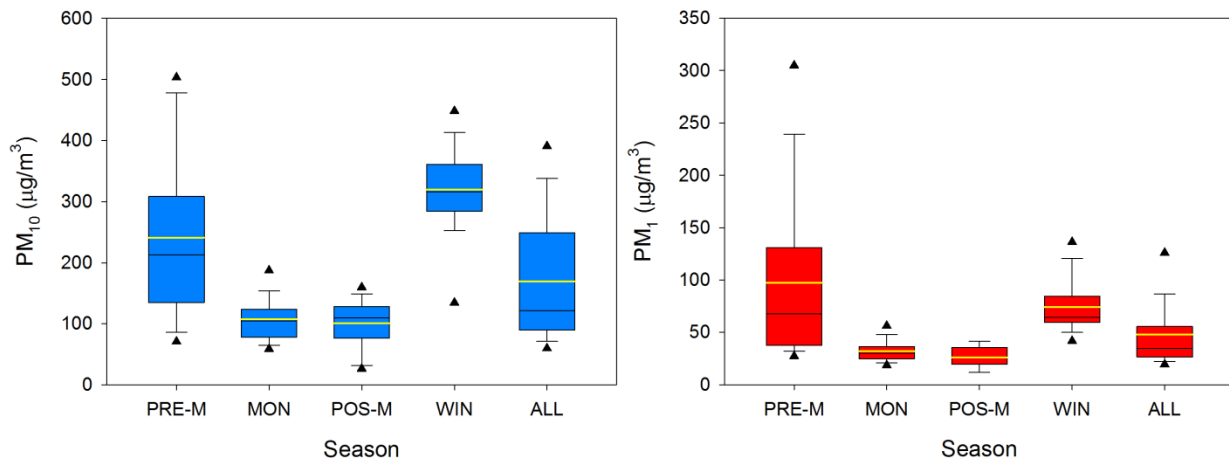


Figure 4. Box and whiskers plot for PM₁₀ (left panel) and PM₁ (right panel) concentrations at Paknajol, segregated by season (PRE-M: Pre-monsoon, MON: Monsoon, POS-M: Post-monsoon, WIN: Winter and ALL: the whole measurement period). The boxes and whiskers denote the 10th, 25th, 75th and 90th percentiles of PM values, triangles denote the 5th and 95th percentiles. The median (mean) value is reported as a black (yellow) line.

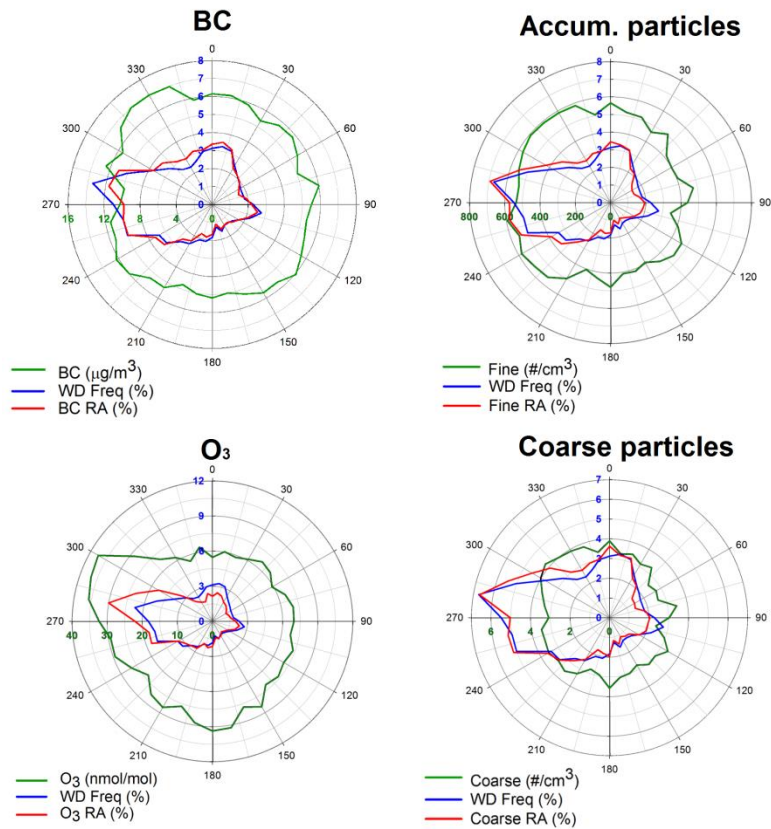


Figure 5. Relation between BC, O₃ (left column), accumulation and coarse particles (right column) and wind direction for Paknajol. The green line represents the mean of respective pollutant per 10° WD interval, the blue line is the relative frequency of WD and the red line is the relative abundance of the chosen pollutant, weighted on the WD frequency, as explained in Gilge et al. (2010).

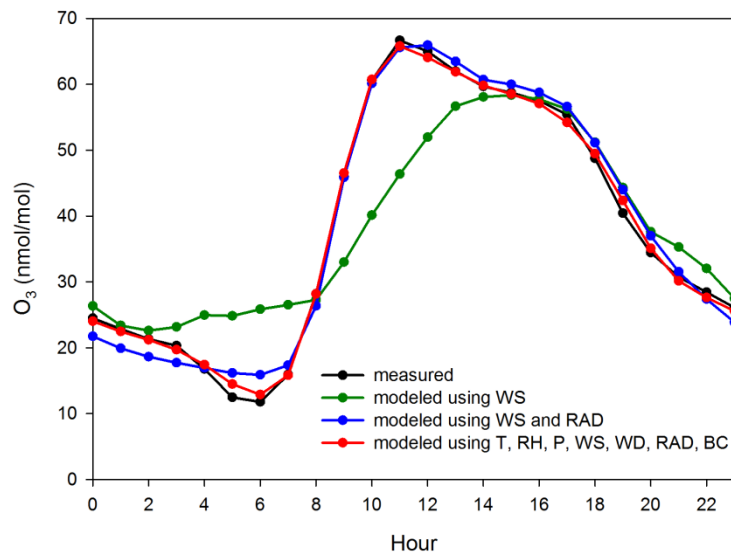


Figure 6. Average seasonal diurnal variation of O₃ concentrations for the pre-monsoon period, compared with modelled O₃ using different input parameters (T, RH, P, WS, WD, RAD and BC).

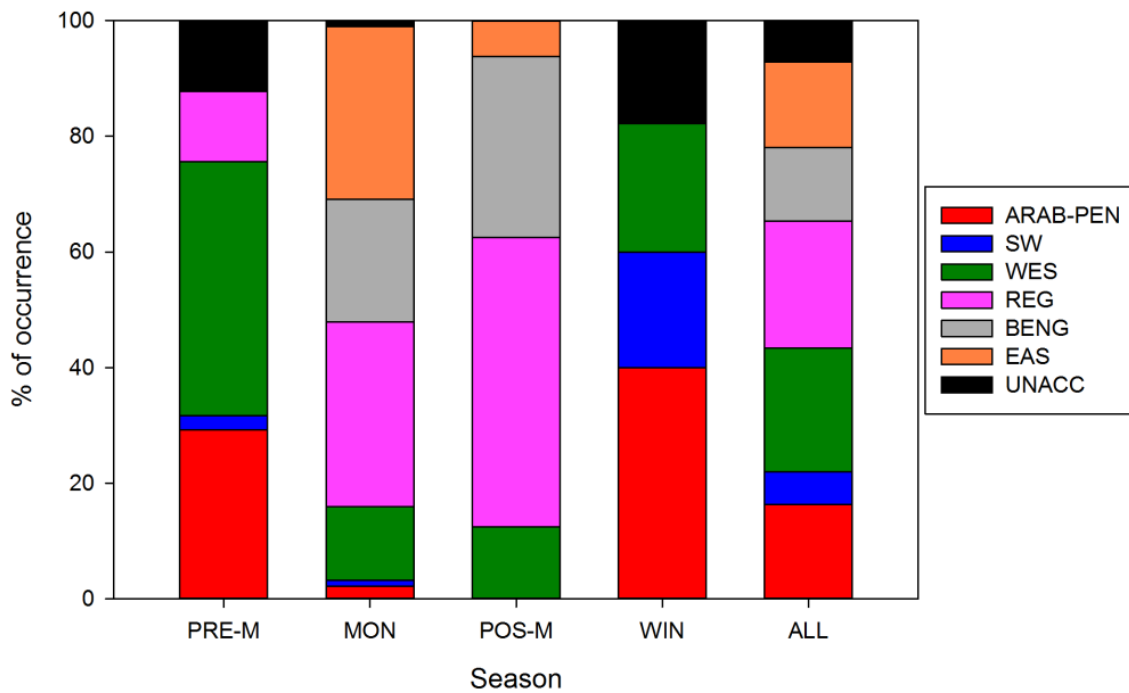


Figure 7. Percentage of occurrence registered by the 6 different back-trajectory clusters considered in this work, divided by season (PRE-M: Pre-monsoon, MON: Monsoon, POS-M: Post-monsoon, WIN: Winter and ALL: considering the whole measurement period). Abbreviations for clusters are the following: ARAB-PEN – Arabian Peninsula, SW – South-westerly, WES – Western, REG – Regional, BENG – Bay of Bengal, EAS – Eastern, UNACC – Unaccounted.

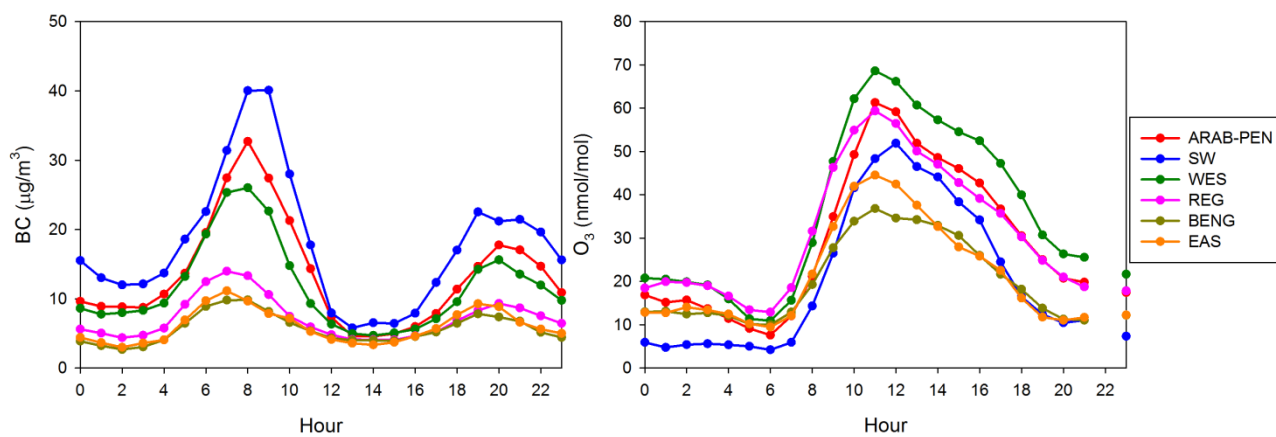


Figure 8. BC (left) and O_3 (right) diurnal variations as a function of the different air-mass clusters shown in Fig. 7. Abbreviations are the following: ARAB-PEN – Arabian Peninsula, SW – South-westerly, WES – Western, REG – Regional, BENG – Bay of Bengal and EAS – Eastern.

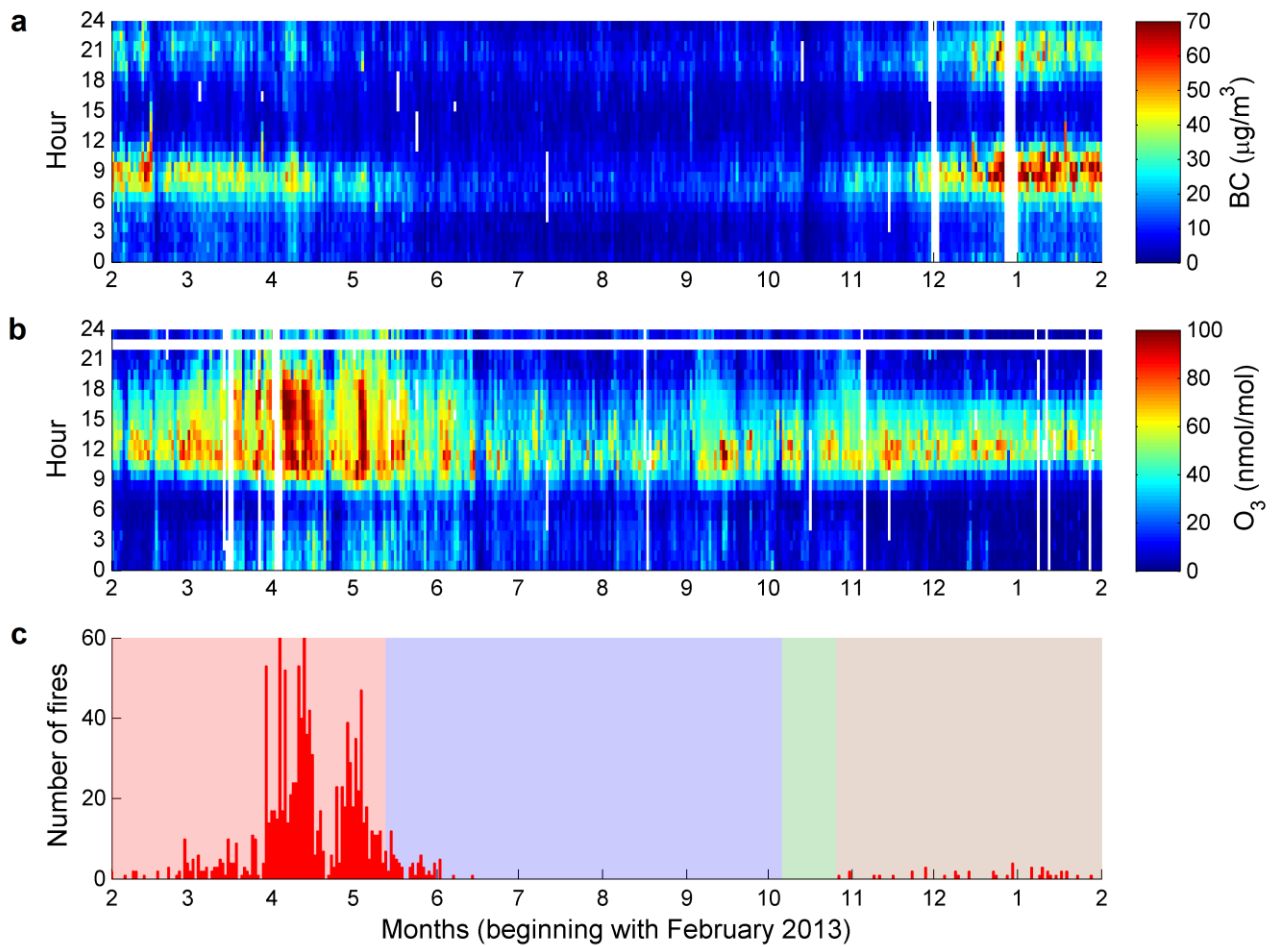


Figure 9. BC (panel *a*) and O_3 (panel *b*) diurnal variations over the entire sampling period. The color scale has been set to a maximum of $70 \mu\text{g}/\text{m}^3$ and $100 \text{ nmol}/\text{mol}$ for BC and O_3 , respectively. Panel *c* shows the total daily number of fires found in the Southern Himalayas box (see Putero et al., 2014); note that the y-axis has been limited to a maximum value of 60. Shaded areas in panel *c* indicate the different seasons (red: pre-monsoon, blue: monsoon, green: post-monsoon and brown: winter).